INFORMATION TO USERS

This manuscript has been reproduced from the microfilm master. UMI films the text directly from the original or copy submitted. Thus, some thesis and dissertation copies are in typewriter face, while others may be from any type of computer printer.

The quality of this reproduction is dependent upon the quality of the copy submitted. Broken or indistinct print, colored or poor quality illustrations and photographs, print bleedthrough, substandard margins, and improper alignment can adversely affect reproduction.

In the unlikely event that the author did not send UMI a complete manuscript and there are missing pages, these will be noted. Also, if unauthorized copyright material had to be removed, a note will indicate the deletion.

Oversize materials (e.g., maps, drawings, charts) are reproduced by sectioning the original, beginning at the upper left-hand corner and continuing from left to right in equal sections with small overlaps.

ProQuest Information and Learning
300 North Zeeb Road, Ann Arbor, MI 48106-1346 USA
800-521-0600

UNIVERSITY OF CINCINNATI

May 15 1950

I hereby recommend that the thesis prepared under my supervision by James G. Kereiakes

entitled EFFECTS OF HIGH PRESSURE AND SHEARING ON POWDERED CRYSTALS IN VACUO

be accepted as fulfilling this part of the requirements for the degree of DOCTOR OF PHILOSOPHY

Approved by: D.A. Wells

FORM 668—G. S. & T. C.—500—5-48

EFFECTS OF HIGH PRESSURE AND SHEARING ON POWDERED CRYSTALS IN VACUO

A dissertation submitted to the

Graduate School of Arts and Sciences

of the University of Cincinnati

in partial fulfillment of the

requirements forthe degree of

DOCTOR OF PHILOSOPHY

1950

by

James G. Kereiakes

B.S. Western Kentucky State College - 1945

M.S. University of Cincinnati - 1947

TABLE OF CONTENTS

INTRODUCTION

The purpose of the work presented in this thesis was (a) to investigate the effects of high pressure alone on certain powdered crystals in a vacuum, and (b) to determine the effects produced on the powdered crystals by oscillating the compressing plunger while, at the same time, the crystals were subjected to pressure.

Most of the work in this general field has, for obvious reasons, been on powdered metals.[1] Elam[2] has summarized the effects of mechanical deformation of the structure and properties of polycrystalline materials as follows:

1. The individual grains become distorted.
2. The deformation takes place by gliding on the crystal planes.
3. The presence of crystal boundaries strengthen the material.
4. The crystals tend to take up certain definite orientations in relation to the deformation.
5. The type of crystal lattice determines the orientation taken up.
6. Mechanical properties are changed by plastic deformation.
7. There is a real hardening of the material, ie., deformation tends to increase the resistance to further deforma-

tion.

8. Change in orientation can only account for part of the effects of mechanical deformation.

Mark, Polanyi, and Sohmid[3] contend that the planes of the crystal are broken up into a system of blocks which are nearly parallel but each block itself being free from distortion. Polanyi is considered one of the pioneers of the crystal distortion field. His researches have appeared from 1922 onwards and are the foundation of the theory of single-crystal deformation.

Considerable work on crystal distortion due to very high pressures has been done by Bridgman[4]. In one of his many works, he found that NaCl, which under normal conditions at atmospheric pressure breaks brittlely in tension on one of its numerous cleavage planes, may be made to support plastic deformation under special conditions, as when properly supported or when in an aqueous solution. He concluded that a crystalline substance, particularly if it is cubic, is more likely to become measureably plastic under pressure than an amorphous substance like glass.

Details of the present investigation now follow.

APPARATUS

COMPRESSION APPARATUS

The assembled apparatus is shown in fig. 1. This, along with the diagram shown in fig. 2, will serve to illustrate the various parts to be discussed.

Hydraulic Press

Pressure was supplied by a laboratory hydraulic press with an available total load of 40,000 pounds. This load when applied to a plunger (die) having a diameter of 1/2 inch provided a maximum pressure of 200,000 pounds per square inch.

Die

The die, made of a chrome-nickel alloy, was oil-hardened to withstand the maximum pressure available from the hydraulic press. The die consisted of three pieces, see fig. 3, and its surfaces were ground and lapped to obtain a fine finish. Four 3/16 inch radial holes through the side piece of the die, D_2, allowed the region containing the crystal powder to be evacuated.

Sylphon Bellows

The sylphon bellows, B_1 and B_2 of fig. 2, allowed for movement of parts of the apparatus without disturbing the vacuum. The vertical bellows, B_1, permitted the movement of the die upon the application of the pressure. The horizontal bellows, B_2, made it possible to oscillate, under pressure, the plunger, D_3 of fig. 3,

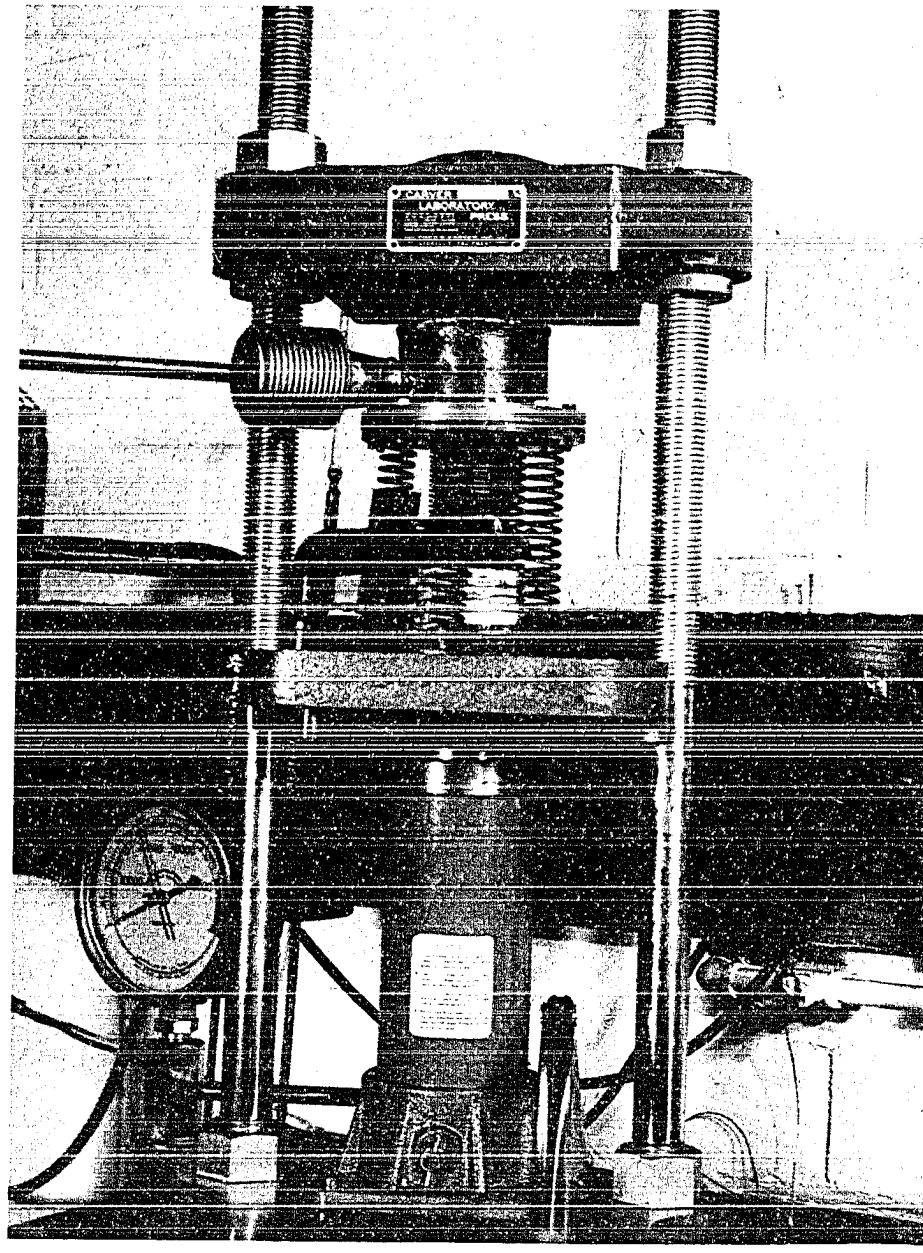

Figure 1

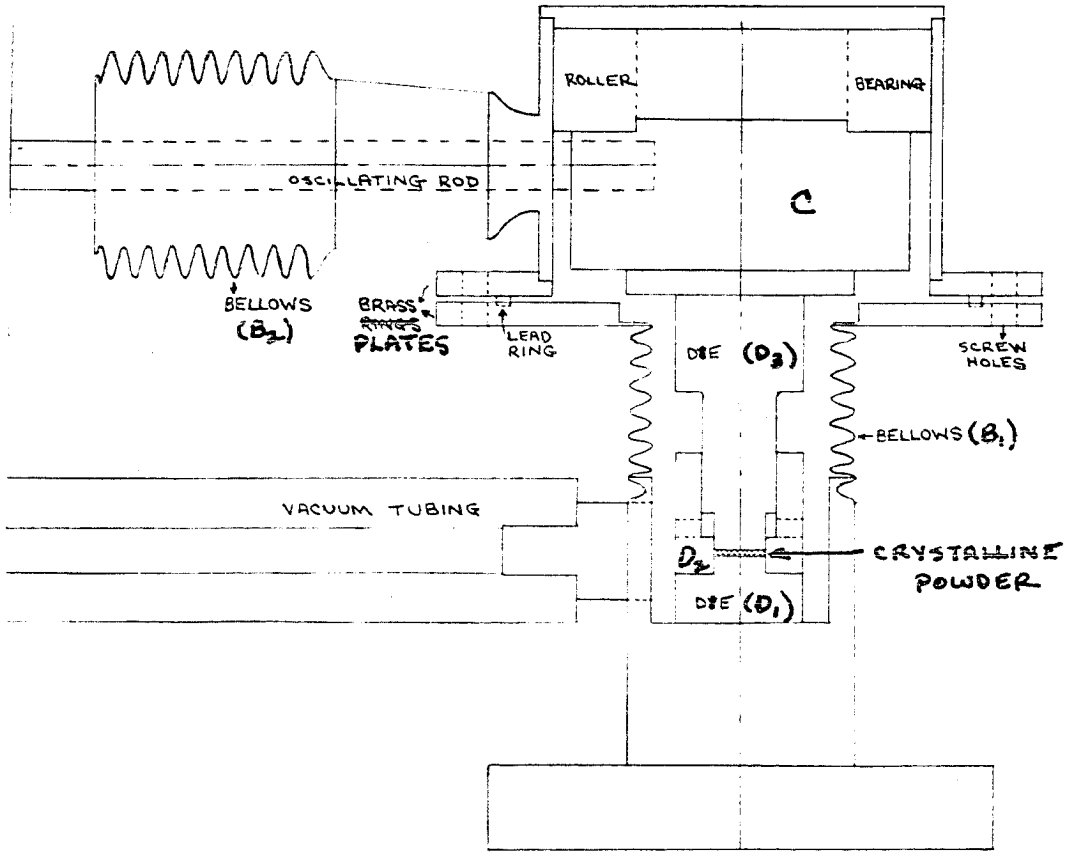

CRYSTAL COMPRESSING APPARATUS

Figure 2

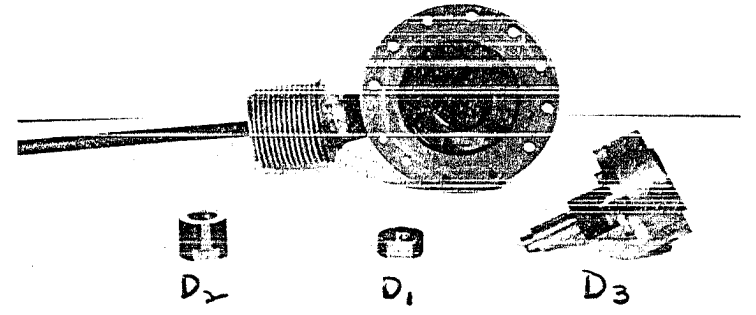

Figure 3

within about ten degrees. It may be mentioned here that with the arrangement of the horizontal bellows as shown, a twisting effect was produced on the bellows causing it to crack under constant use. Hence it was necessary to replace this bellows from time to time.

Roller Bearing

A large roller thrust bearing, capable of withstanding a total force of 40,000 pounds, was placed as shown in fig. 2. This made it possible to oscillate the plunger under the high pressures used.

Springs

The upper portion of the apparatus was supported by springs, see fig. 1, and prevented the vertical bellows from collapsing under atmospheric pressure. Their length was such as to keep the plunger above the vacuum holes in the side piece of the die, D_2, so that region containing crystal powder may be evacuated.

Oscillating Lever

The oscillation under pressure was accomplished with a 1 1/2 foot lever connected through the horizontal bellows to the steel cylinder, C of fig. 2, that is screwed with the plunger. Total angle through which the plunger could be rotated was about 10°.

Vacuum System

The vacuum system is shown in fig. 4. Two pumps were used in tandem. A large megavac forepump was connected through copper tubing to a water-cooled, all-metal, two-stage, oil diffusion pump. Heavy rubber vacuum tubing connected the oil diffusion pump with the compression apparatus.

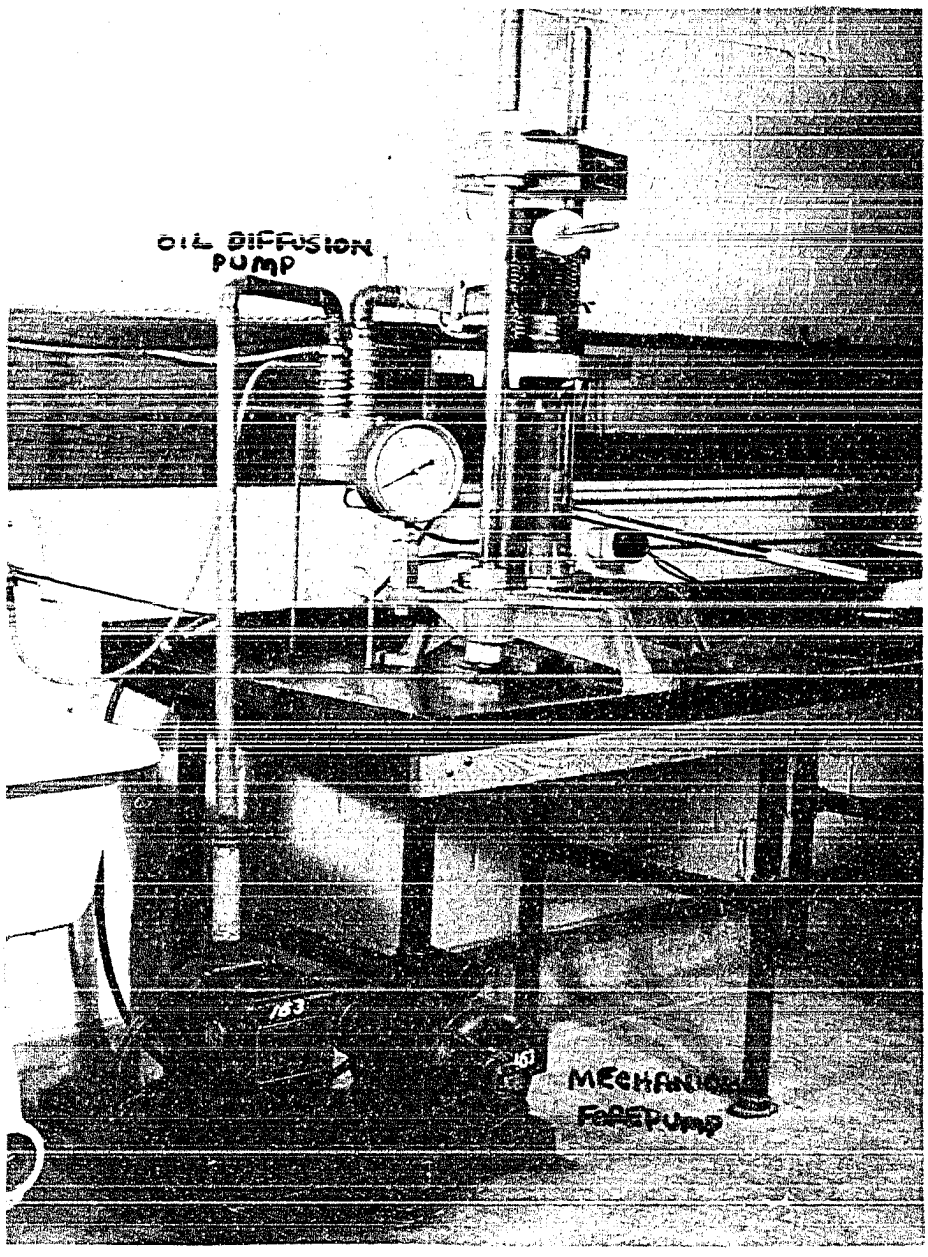

Figure 4. Vacuum System

The upper part of the apparatus was fastened to the lower part by bolting two brass plates together as shown in fig. 2. This connection was made vacuum tight by means of a lead ring placed between the two brass plates. The bottom plate contained a small groove into which the lead ring was placed, after first covering the bottom of the groove with glyptal to insure a better seal. The top brass plate was tightened over the lead ring by twelve screws placed symmetrically around the edge of the brass plates. This ring seal was the means by which samples (as well as internal parts) were introduced and removed.

A Tesla coil applied to a discharge tube, placed between the diffusion pump and the compression apparatus, supplied general information concerning the vacuum condition.

The purpose of the vacuum system was to eliminate most of the moisture and occluded gases in the powdered crystals. It has been found that crystals compressed at atmospheric pressure never become completely clear.

ANALYSIS APPARATUS

X-Ray Diffraction Equipment

The compressed samples were analyzed with the North American Phillips X-Ray Diffraction Machine shown in fig. 5. The machine contains four window outlets, and permitted four pictures to be taken simultaneously. A molybdenum target tube, operated at 50 kilovolts and 18 milliamps was used. A zirconium filter eliminated practically all radiation except the desired k_{α} line of molyb-

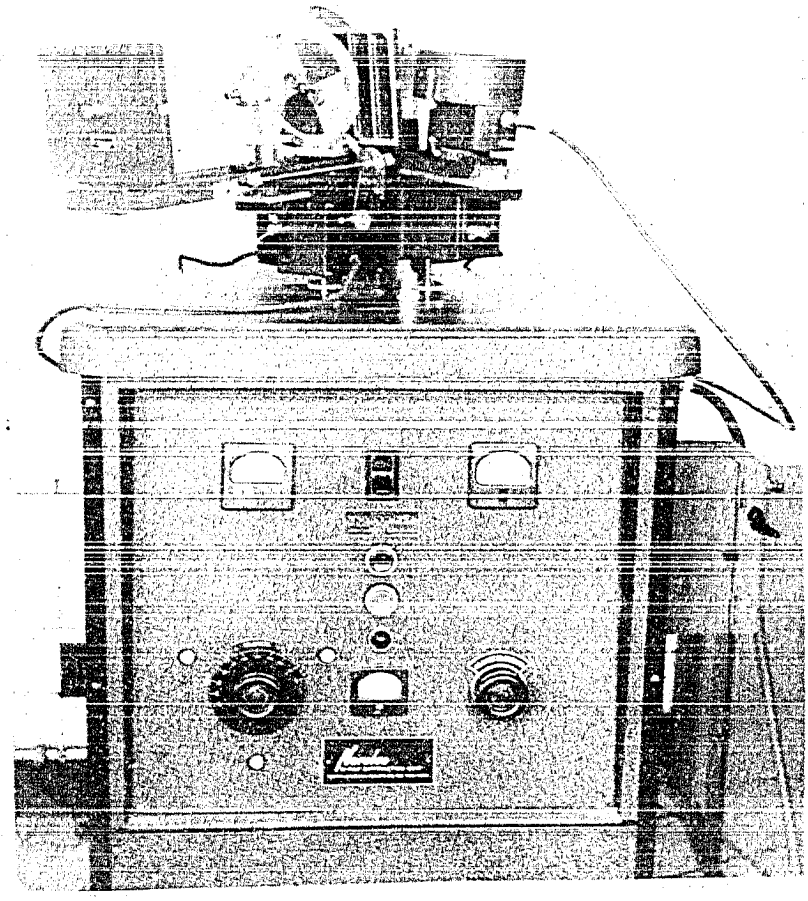

Figure 5. X-Ray Diffraction Machine

denum.

The pinhole transmission camera shown in fig. 6 was used for general investigations of the compressed samples. Four of these were constructed and used simultaneously to take advantage of the four window outlets of the tube. The x-ray film was contained in a light-tight envelope. A lead piece attached to the envelope served to remove the main beam.

The diffraction patterns contained in this thesis were taken with the flat camera shown in fig. 7. It incorporates two film cassettes (for transmission and back reflection), a specimen holder, a collimating system, and a beam removal tube, all supported on a machined track. Use was made only of the transmission cassette, which was mounted to a holder longitudinally translatable along the track. A specimen post is mounted on the track carriage, permitting the attainment of a desired relationship between the specimen and the transmission cassette. A one mm. pinhole was used in the collimating system.

The diffraction patterns were taken with Kodak medical x-ray film and were developed and fixed with liquid x-ray developer and fixer respectively.

Microphotometer

The sharp ring diffraction patterns were further investigated with a Zeiss microphotometer. Super panchro-press type B film was used and developed with DK 60 A.

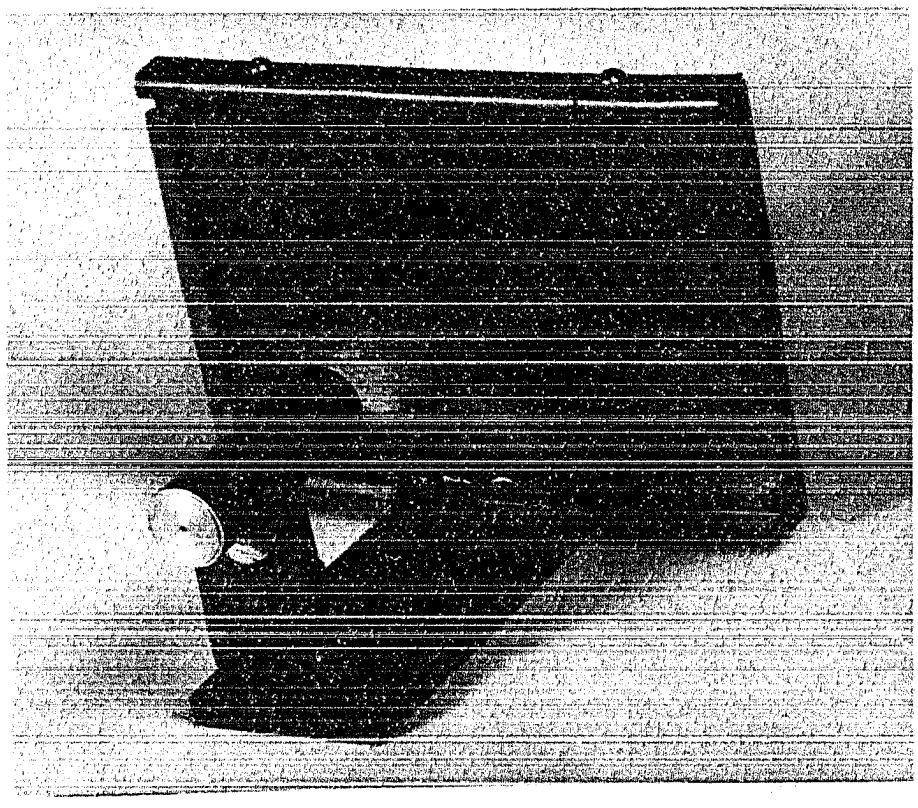

Figure 6. Crude Pinhole Camera

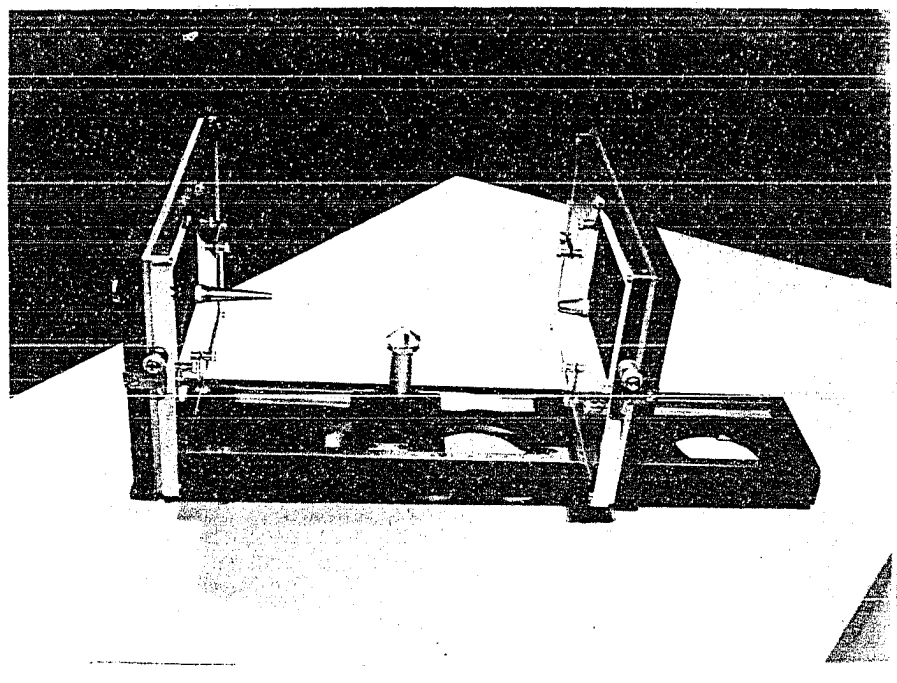

Figure 7. Flat Camera

GENERAL PROCEDURE

The potassium chloride was first ground in a mortar to a fine powder and passed through a sieve to obtain a fairly uniform grain size of between 60-80 microns.

About .1 gram of the fine powder was placed on the top surface of die piece, D_1. This was then located inside of the apparatus as shown in fig. 2 and the supporting springs set up. The top part of the apparatus (including the roller bearing, steel piece with the oscillating lever, horizontal bellows, the plunger, and the top brass plate) was adjusted in place. After the screws were tightened to insure a good vacuum seal, the mechanical forepump was operated for about 10 minutes; after which the oil diffusion pump was put into operation and the pressure maintained at about 10^{-4} mm. Hg for about 15 minutes before compressing the powdered crystal.

The pressure was then applied as stated below. The resulting sample (in the form of a hardened disc of 1/2 inch in diameter and from 13-18 mils thick) was then analyzed by x-ray diffraction methods.

Compression Alone

Samples were subjected to pressures (without oscillation) ranging from 5,000 lbs./in^2 to 200,000 lbs./in^2 The time of compression was retained at approximately two minutes throughout, although experimentation proved the time element was not critical.

Compression with Oscillation

Samples were then made by oscillating the plunger while the powder was subjected to pressure. Six samples were thus made at a constant pressure of 50,000 lbs./in.^{2} and for 1, 3, 5, 10, 20, and 40 oscillations of the plunger respectfully.

Six samples were made for a constant number of 40 oscillations of the plunger and for pressures of 5,000, 10,000, 20,000, 30,000, 40,000, and 50,000 lbs./in.^{2}, respectively.

Analysis of Samples

X-ray diffraction patterns of the above samples were made with the surface of the sample perpendicular to the undeviated x-ray beam. The sharp ring diffraction patterns required further analysis with a microphotometer.

Diffraction pattern of a sample of KCl compressed at 50,000 lbs./in.^{2} and for 40 oscillations of the plunger was further analyzed for the purpose of determining the preferred orientation. Films were taken with the surface of the sample rotated at different angles, $0°$-$50°$ in steps of $10°$, with respect to the undeviated x-ray beam. The specimen holder of the flat camera was of such type that allowed rotation of the sample about a vertical axis to desired angle without requiring its removal from the holder or the removal of the holder from its position.

Diffraction patterns were taken of samples of KCl, NaCl, and KBr (compressed under the same conditions of 50,000 lbs./in.^{2} and for 40 oscillations of the plunger).

INTERPLANAR SPACING

The x-ray pattern produced on the film was a series of Debye rings which were concentric with the undeviated x-ray beam.[5] The angle between the incident x-ray beam and the family of crystal planes which reflect to form the particular Debye circle under consideration is called θ and is given by the relation

$$\tan 2\theta = \frac{r}{D} \qquad (1)$$

where r is the radius of the Debye ring and D is the perpendicular distance from the sample to the film. The interplanar spacing may be found from Bragg's Law

$$n\lambda = 2d \sin \theta \qquad (2)$$

where λ is the wavelength of x-radiation used, n is the order of the diffraction ring, θ is the angle mentioned above and referred to as the Bragg angle of incidence.

A spacing value is obtained for each Debye ring and denotes essentially the distance between the family of planes which reflect to form the particular Debye ring. For a cubic system, the interplanar spacing, d, is given by

$$d = \frac{a_o}{\sqrt{h^2 + k^2 + l^2}} \qquad (3)$$

where h, k, l are the Millerian indices of planes, and a_o is the length of one cell of atomic structure of the crystal.

The values of thirteen interplanar spacings of KCl as obtained from the overexposed diffraction pattern of fig. 8 are given in fig. 9. The sample to film distance was 4.95 cm. and the x-radiation was molybdenum K_{α} .707 Angstrom units. The interplanar spacings were found to agree very closely with those given by SPROULL.[5]

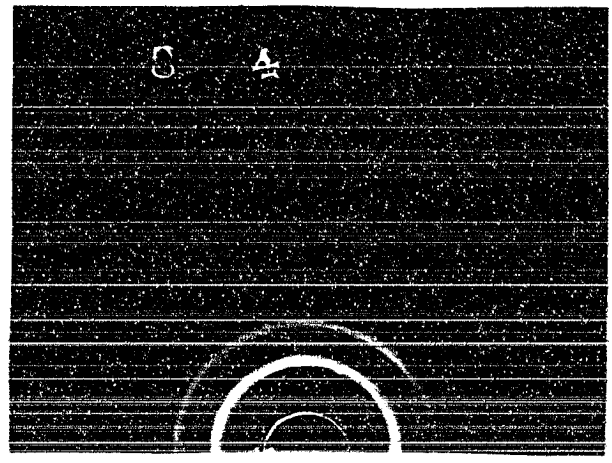

Figure 8

x	tan 2θ	θ	sin θ	d A.U.
1.135	.2295	6 27.5'	.11248	3.140
1.638	.3308	9 9 '	.15902	2.220
2.040	.4120	11 11.5'	.19409	1.820
2.412	.4870	12 59 '	.22467	1.572
2.760	.5580	14 34.5'	.25165	1.402
3.085	.6235	15 58.5'	.27522	1.262
3.720	.7520	18 26' '	.31675	1.115
4.075	.8240	19 44.5'	.33778	1.045
4.410	.8915	20 51.5'	.35606	.994
4.750	.9600	21 55 '	.37326	.948
5.125	1.0350	22 59.5'	.39060	.905
5.500	1.1110	24 .5'	.40687	.870
5.850	1.1810	24 52.5'	.42064	.841

ANALYSIS OF COMPRESSED SAMPLES

Samples compressed at pressures of 5,000, 10,000, 20,000, 30,000, 40,000, 50,000, 100,000, 150,000, and 200,000 lbs./in.^{2}, respectively, are shown in fig. 10. It is seen that the samples are in the form of hardened disks 1/2 inch in diameter and about 15-18 mils thick. The general appearance of the compressed samples ranges from a white disk to a completely transparent disk at around 125,000 lbs./in.^{2}

The x-ray diffraction patterns of powdered KCl and of the KCl samples compressed under above mentioned pressures are shown in fig. 11-16. These were taken with the x-ray beam directed through the sample near its edge; the reason for this will become evident later.

The powder sample gives a spotty pattern, fig. 11, indicating a large grain size (60-80 microns as determined from sieve). Fig. 12 for pattern of a sample compressed at 5,000 lbs./in.^{2} snows fewer spots indicating a decrease in grain size. Fig. 13 shows that 10,000 lbs./in.^{2} is sufficient, to give sharp rings which indicate a grain size slightly less than 5×10^{-3} mm. The remaining fig. 13-15 show that with additional pressure the rings remain sharp.

Theoretically,[5] as the grain size continues to decrease to below 2×10^{-4} mm., the rings in the pattern begin to lose their sharpness and show signs of broadening and "fuzziness", because such crystals lack the necessary resolving power to produce sharp rings.

Since this broadening of the rings on the diffraction patterns

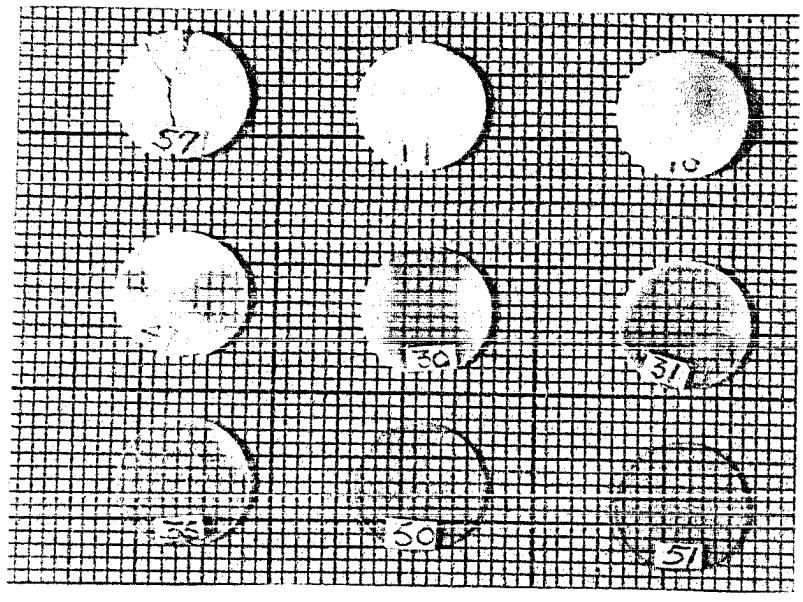

Figure 10. Samples Compressed Only

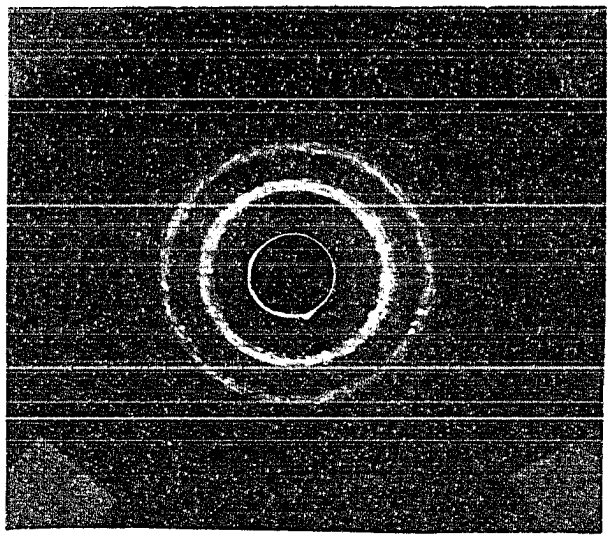

Figure 11. X-Ray Diffraction Pattern of KCl Powder

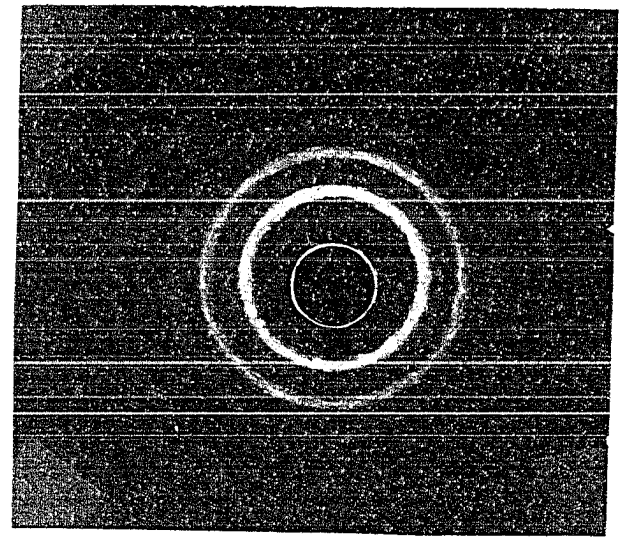

Figure 12. Pattern of KCl Sample Compressed at 5,000 lbs./in^2

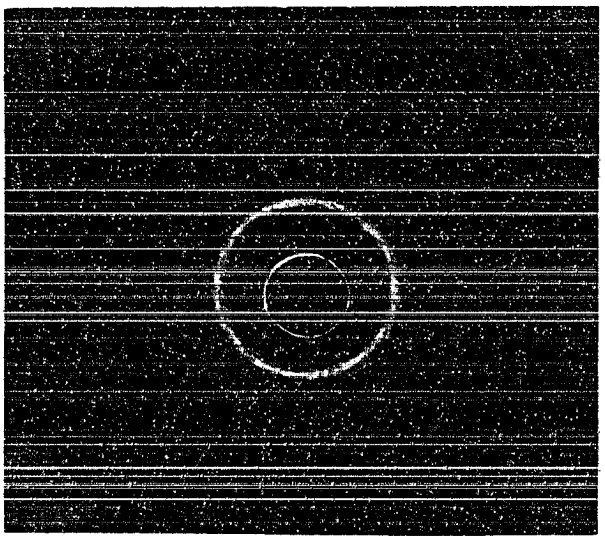

Figure 13. Pattern of KCl Sample Compressed at 10,000 lbs./in^2

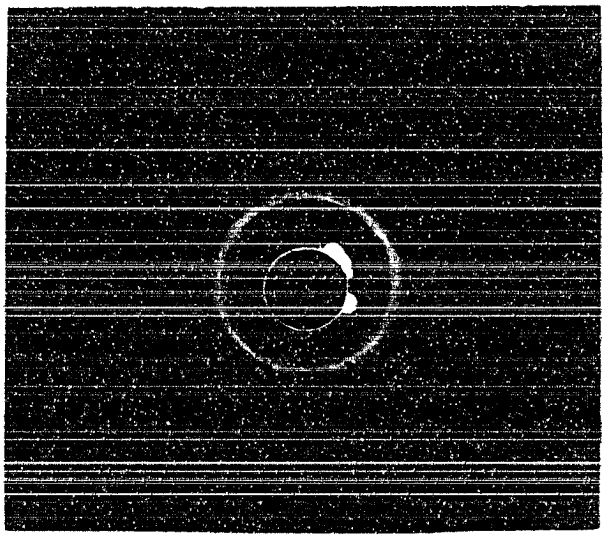

Figure 14. Pattern of KCl Sample Compressed at 50,000 lbs./in^2

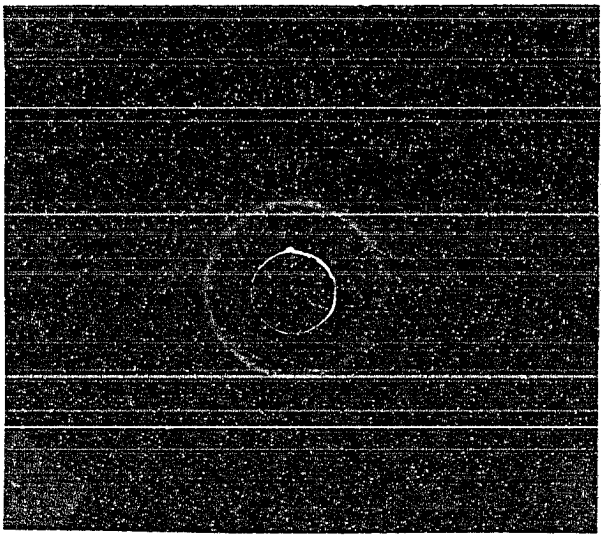

Figure 15. Pattern of KCl Sample Compressed at 100,000 lbs./in^2

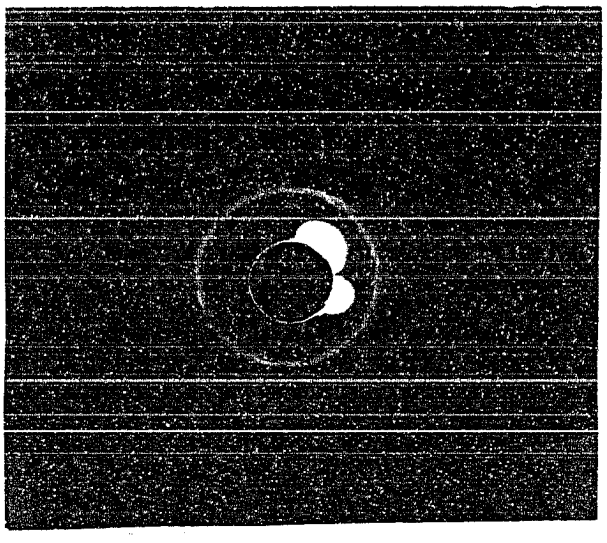

Figure 16. Pattern of KCl Sample Compressed at 200,000 lbs./in^2

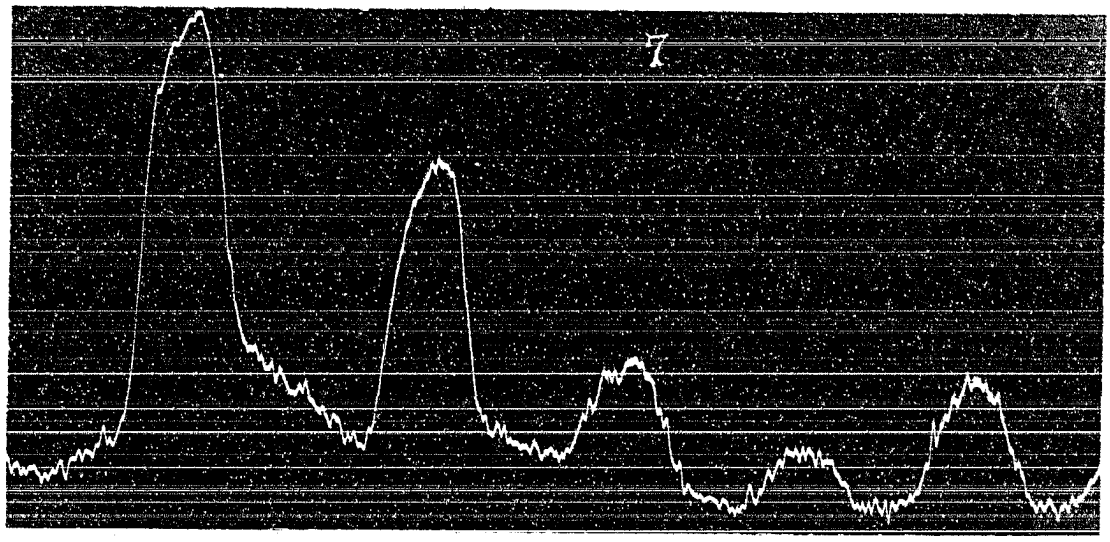

Figure 17. Microphotometer Film of Pattern of KCl Sample Compressed at 10,000 lbs/in.^{2}

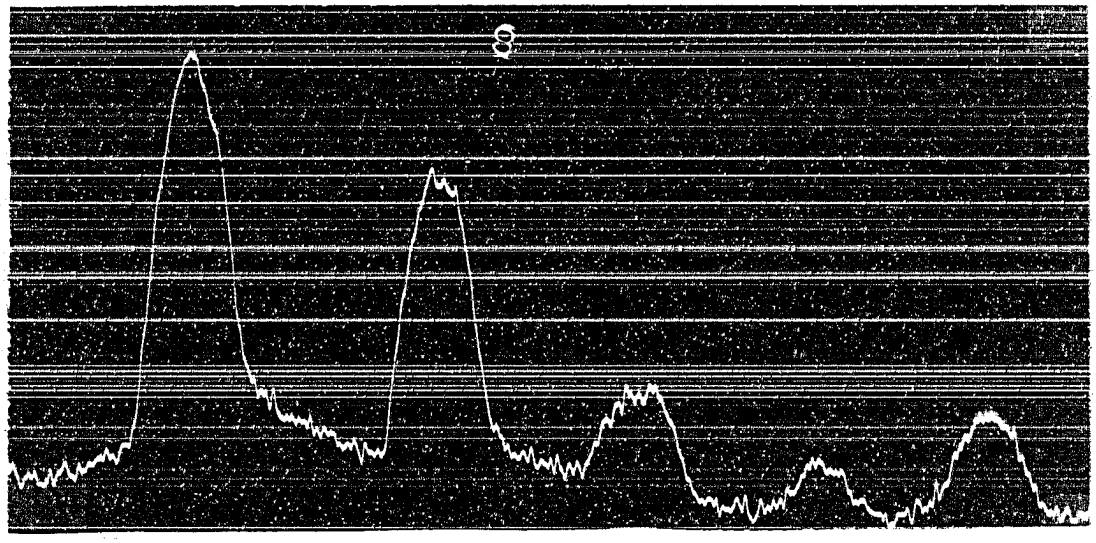

Figure 18. Microphotometer Film of Pattern of KCl Sample Compressed at 100,000 lbs/in.^{2}

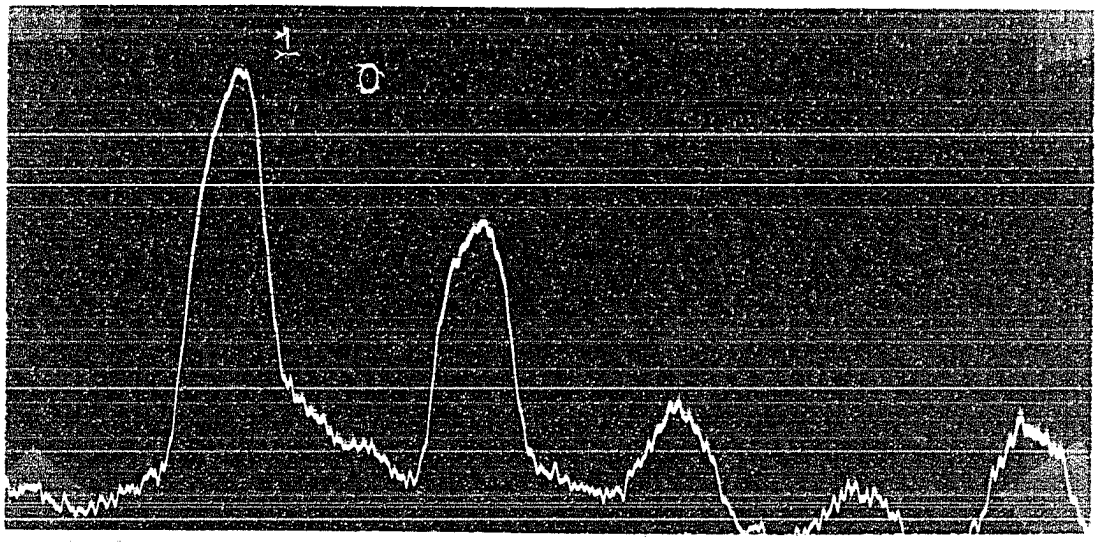

Figure 19. Microphotometer Film of Pattern of KCl Sample Compressed at 200,000 lbs/in.^{2}

was not evident by the eye, the patterns were further investigated with a microphotemeter. The results for the diffraction patterns for the 10,000 lbs./in.^{2}, 100,000 lbs./in.^{2}, and 200,000 lbs./in.^{2} compressed samples are shown in fig. 17-19. These intensity films superimpose on each other and indicate no appreciable line broadening.

Sproull states that between 5×10^{-3} mm. and 2×10^{-4} mm., the x-ray pattern is insensitive to grain size. Therefore when a sample yields a sharp ring pattern, one can only say that its grain size lies within this range. Grain size of samples compressed from 10,000-200,000 lbs./in.^{2} must lie between 5×10^{-3}mm. and 2×10^{-4} mm.

It can also be concluded from the fact that the Debye rings retained uniform density throughout this phase of the investigation, no preferred orientation seemed to appear in the samples compressed only.

ANALYSIS OF SAMPLES COMPRESSED WITH OSCILLATION OF PLUNGER

It was found that with oscillation of the plunger while the sample is subjected to pressure, the sample became completely transparent at a pressure of around 40,000 lbs./in.^{2}, as compared to around 125,000 lbs./in.^{2} required for complete clearness for compression alone. The explanation may be that the oscillatory motion of the plunger aided in filling in the microscopic voids more effectively than the compression alone. If this is to be true, then the thickness of the samples for each case should vary. Actual measurements of some of the samples revealed that the thickness of the samples obtained with oscillation of the plunger were around 2 mils thinner than samples obtained by compression only.

X-ray diffraction patterns of the samples compressed with oscillation of the plunger proved very interesting. When the x-ray beam was directed through the center of the sample, a sharp ring pattern, similar to one for compression only, was obtained (indicating that here the oscillatory motion had no effect). But when the x-ray beam was directed through the sample near its edge, the pattern indicated that the oscillatory motion introduced a preferred orientation, evident from the enhanced arcs on the Debye ring. So in this work on preferred orientation, the patterns were taken with the x-ray beam directed through the sample near its edge.

Fig. 20-25, showing the effect of 1, 3, 5, 10, 20, and 40 oscillations of the plunger, respectively, for a constant pressure of 50,000 lbs./in^2, indicate that an increase in the degree of preferred orientation is taking place. More than 40 oscillations of the plunger, under the conditions of the present experiment, did not seem to change appreciably the degree of preferred orientation.

Samples compressed for varying pressures of 5,000, 10,000, 20,000, 30,000, 40,000, and 50,000 lbs./in^2, respectively, and for a constant 40 oscillations of the plunger are shown in fig. 26. Here it is evident that the sample becomes completely transparent at around 40,000 lbs./in^2. Fig. 27-32, showing the effect of increasing the pressure from 5,000-50,000 lbs./in^2 for a constant 40 oscillations of the plunger, indicate an increase in the degree of preferred orientation. Oscillation of the plunger at pressures above 50,000 lbs./in^2 usually injured the horizontal bellows, thus limiting this phase of the investigation.

An important point which should be mentioned is the following. When the x-ray beam was directed through the sample near its edge at some point A, as shown below, a pattern similar to fig. 32 was obtained. When the beam was directed through some point B (see below), the same pattern was displaced in respect to pattern obtained for point A. If, however, the sample was rotated so that point B coincided with the original point A position, a pattern similar to one for original point A was repeated with no

displacement. This indicated symmetry in the samples. The reference direction selected for the ensuing work on preferred orientation was the direction of shear. As is evident from the diarams below, this direction is perpendicular to the radius of the sample. The patterns in this work were obtained with the x-ray beam directed through a point coinciding with A in the diagram below.

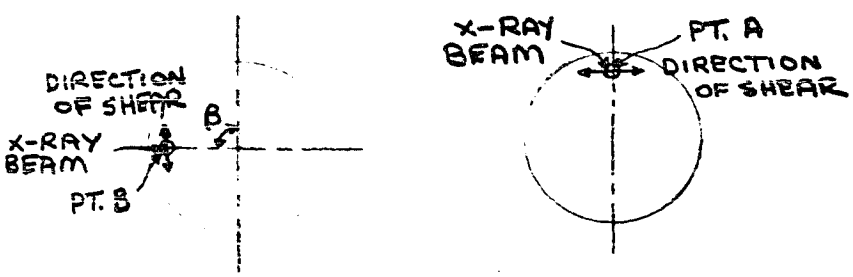

X-RAY DIFFRACTION PATTERNS OF KCl SAMPLES COMPRESSED AT 50,000 lbs./in.^{2} FOR VARIOUS OSCILLATIONS OF PLUNGER

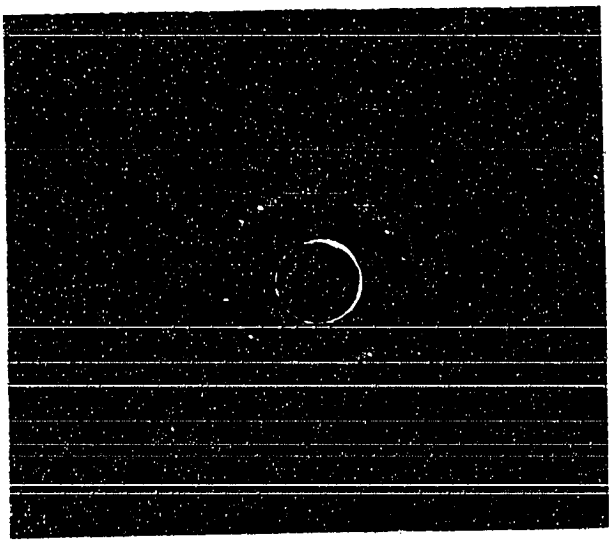

Figure 20. One oscillation

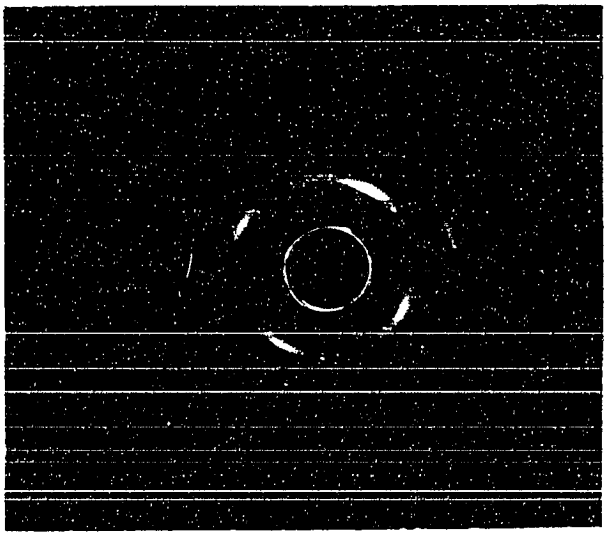

Figure 21. Three oscillations

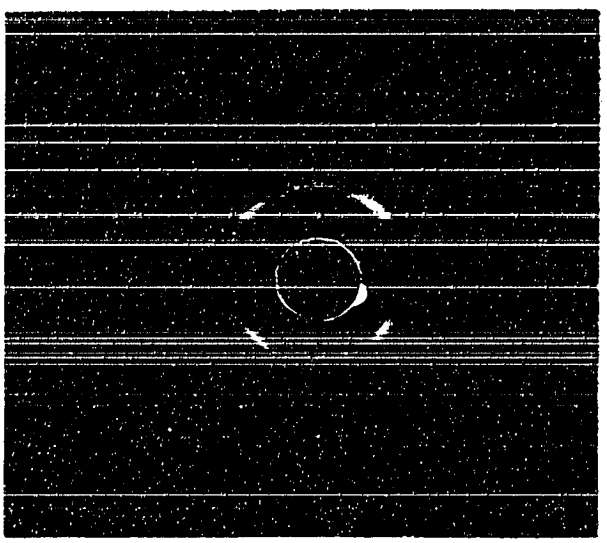

Figure 22. Five oscillations

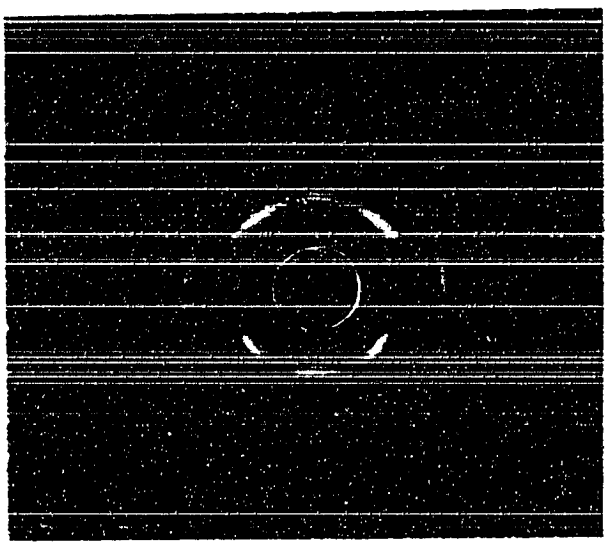

Figure 23. Ten oscillations

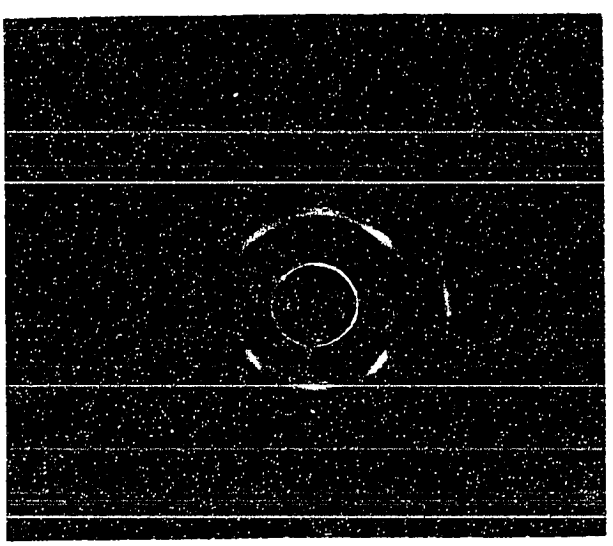

Figure 24. Twenty oscillations

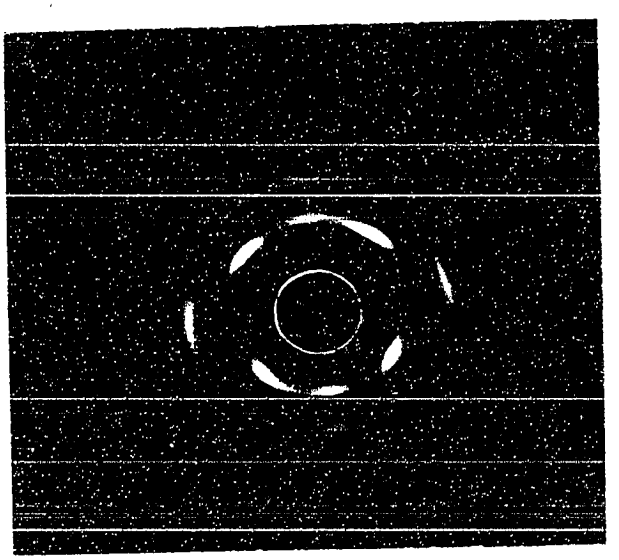

Figure 25. Forty oscillations

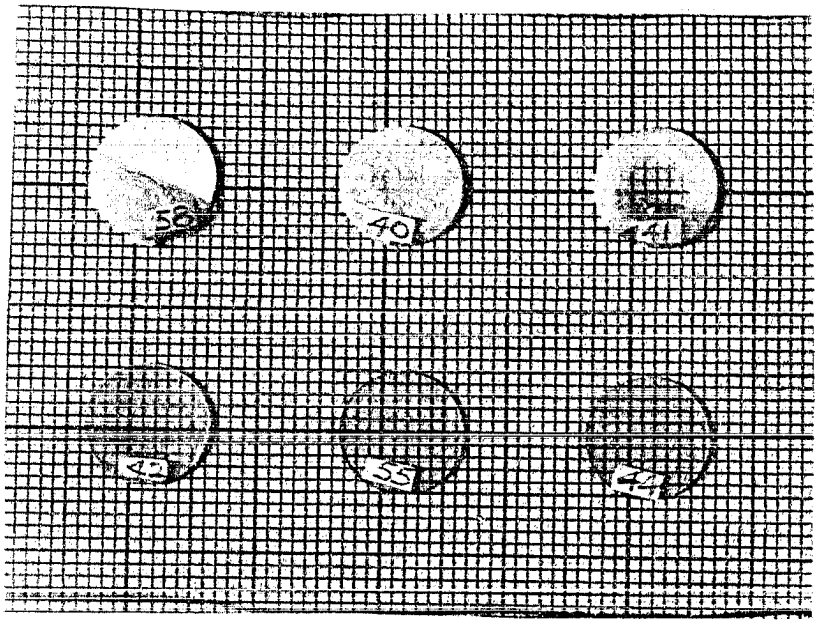

Figure 26. KCl Samples Compressed With Constant No. of Oscillations of Plunger for various pressures

X-RAY DIFFRACTION PATTERNS OF KCL SAMPLES COMPRESSED WITH CONSTANT NUMBER OF OSCILLATIONS OF PLUNGER FOR VARIOUS PRESSURES

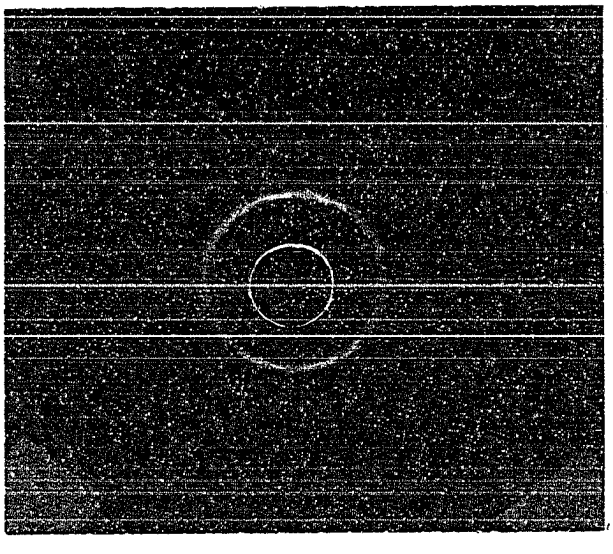

Figure 27. 5,000 lbs./in.^{2}

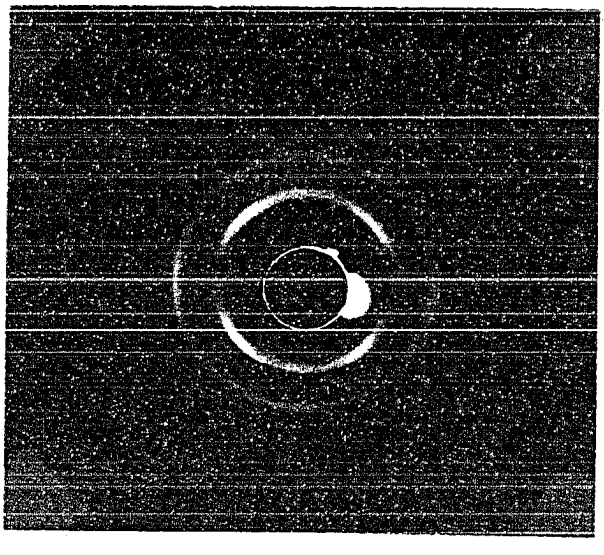

Figure 28. 10,000 lbs./in.^{2}

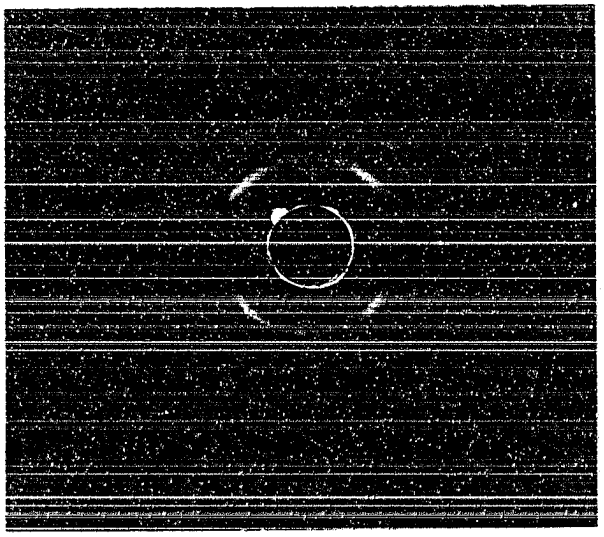

Figure 29. 20,000 lbs./in^2

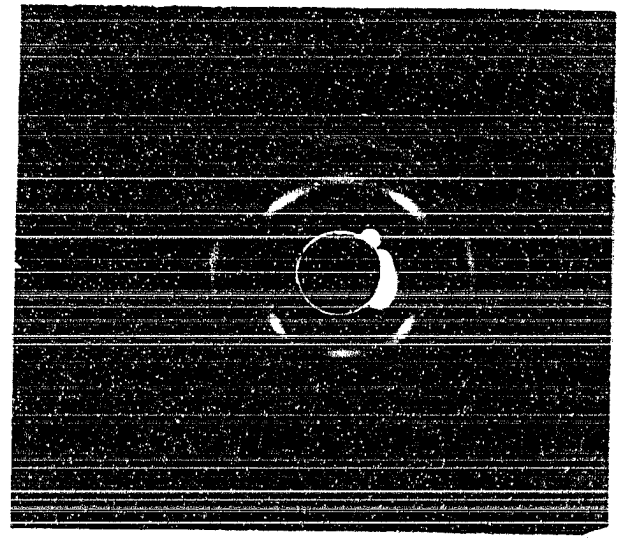

Figure 30. 30,000 lbs./in^2

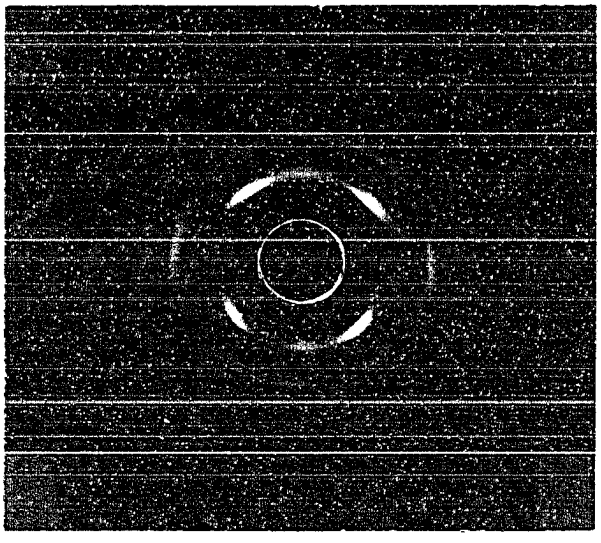

Figure 31. 40,000 lbs./in^2

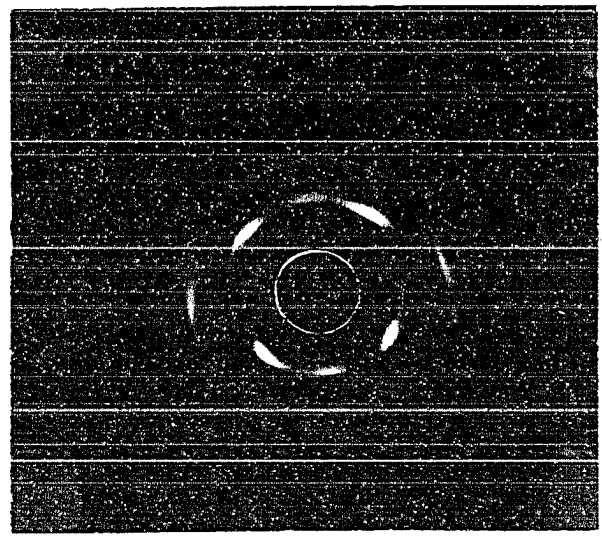

Figure 32. 50,000 lbs./in^2

PREFERRED ORIENTATION

Preferred orientation results from the tendency of the crystals to glide or slip along certain crystallographic planes.[7] Such planes of slip are usually among the most densely populated sets, ie., sets of planes having more atoms per unit area than other crystallographic planes. The special directions of fragmentation and slip results in the fragments acquiring preferred orientation with respect to certain directions of the working process, ie., with the direction of shear in this case.

This preferred orientation may be beneficial or detrimental. N. Goss,[8] has found that the electrical properties of silicon sheet steel for transformer laminae are improved by allowing it to retain its preferential orientation. Such steel has a considerably higher magnetic permeability in the direction of roll. J. Snoek[9] has found that the resistance of nickel steel to corrosion improves when the orientation is preferential. In general, however, preferred orientation is objectionable, because it weakens a metal and reduces its ability to withstand further deformation.

The intensity of the Debye ring will range from uniform density for completely random orientation of the crystalline grains in the sample to spots of maximum density separated by regions of zero density for perfect orientation of a single crystal sample.[10] The KCl sample compressed with oscillation of the plunger contains

an unknown condition of preferred orientation between that of a single crystal and random orientation. Therefore, the intensities of the Debye ring will range between above-mentioned limits (see fig. 32). Regardless of the crystalline orientations present in the sample, the intensity at any one point of the Debye ring is proportional to the number of planes which are in a position to reflect rays to the point.

It must now be attempted to correlate the positions of the enhanced arcs or spots of the Debye rings with the chosen axis of reference of the specimen.

Consider a crystallographic plane whose normal NO makes an angle α with the vertical axis of the sample (see fig. 33). A crystallographic plane will be in position to satisfy the Bragg condition, and a reflection will occur to give a spot on the appropriate Debye ring, the azimuthal position φ at which it occurs being a function of α and the Bragg angle θ.

If α is 90° the crystallographic plane lies parallel to the axis (vertical), in which case only two spots can appear on the end points of the horizontal axis. If the normal of the crystallographic coincides with the axis of the sample, the x-ray beam will lie in the crystallographic plane and the condition for a reflection will never be attained. There is also the possibility that α will just equal the Bragg angle θ. In such a case $\varphi = 0$ and two reflection spots appear diametrically opposite each other on the vertical axis.

It is evident then that the orientations of the lattice planes in the specimen can be found by measuring the azimuthal positions of the intensity maxima in the Debye arc. The relation between θ, α, and φ takes a very simple form

$$\cos \varphi = \frac{\cos \alpha}{\cos \theta} \qquad (4)$$

which may be obtained readily by use of spherical trigonometry.

With hard radiation such as MoK_α used in this case, the reflection angles θ for low orders are small. Hence, we may write $\varphi = \alpha$, since in such cases cosine θ is approximately one.

From the diffraction pattern, a list of reflection haloes and approximate values of φ for the positions of the intensity maxima in the intensified arcs is obtained. To determine from the φ's which crystallographic axis (uvw) lies parallel to the axis, it is required to know the angle between the normal to the lattice plane (hkl) and the zone axis (uvw). For a cubic lattice, this angle is given by

$$\cos \alpha = \frac{uh + vk + wl}{\sqrt{h^2 + k^2 + l^2}\ \sqrt{u^2 + v^2 + w^2}} \qquad (5)$$

Values of α for the (100) and the (110) lattice planes obtained from Bozorth[12] are given below.

	Zone Axis	
Lattice Plane	100	110
100	0, 90	45, 90
110	45, 90	0, 60, 90

Fig. 32 shows a diffraction pattern of a KCl sample compressed with oscillation of the plunger taken with MoK_α radiation. It will be observed that radial streaks extend outwards from the center towards each reflection arc on the Debye rings. These are produced by the continuous, or white radiation, which is reflected mirror-like from the preferentially oriented lattice planes.[13] The effect of varying wavelength is to change all the dimensions of the figure which otherwise retains the same symmetry. The white radiation has its peak value at .4 Angstrom unit. It therefore produces a streak pointing towards each spot formed by the MoK_α line with a wavelength .707 Angstrom unit.

The innermost halces of fig. 32 are the 100 and 110 reflections. If a horizontal axis, corresponding to the direction of shear, is selected as a reference, angles φ for the 100 reflections are 45° and 90°. Either from equation (5) or table above, for φ angles of 45° and 90° related to the plane, we find them against zone axis (110). Hence the (110) axes are parallel to the direction of shear. For the 110 reflection we obtain φ angle values of 0°, 60°, and 90°. From table we again find that (110) zone axis will give these direction values. This confirms that the (110) lattice direction lies parallel to the direction of shear.

However, the above gives no detailed or overall information as to the character and degree of preferred orientation. Only feasible method for studying preferment in this manner is to make a pole figure for the specimen. Such a pole figure is a summary

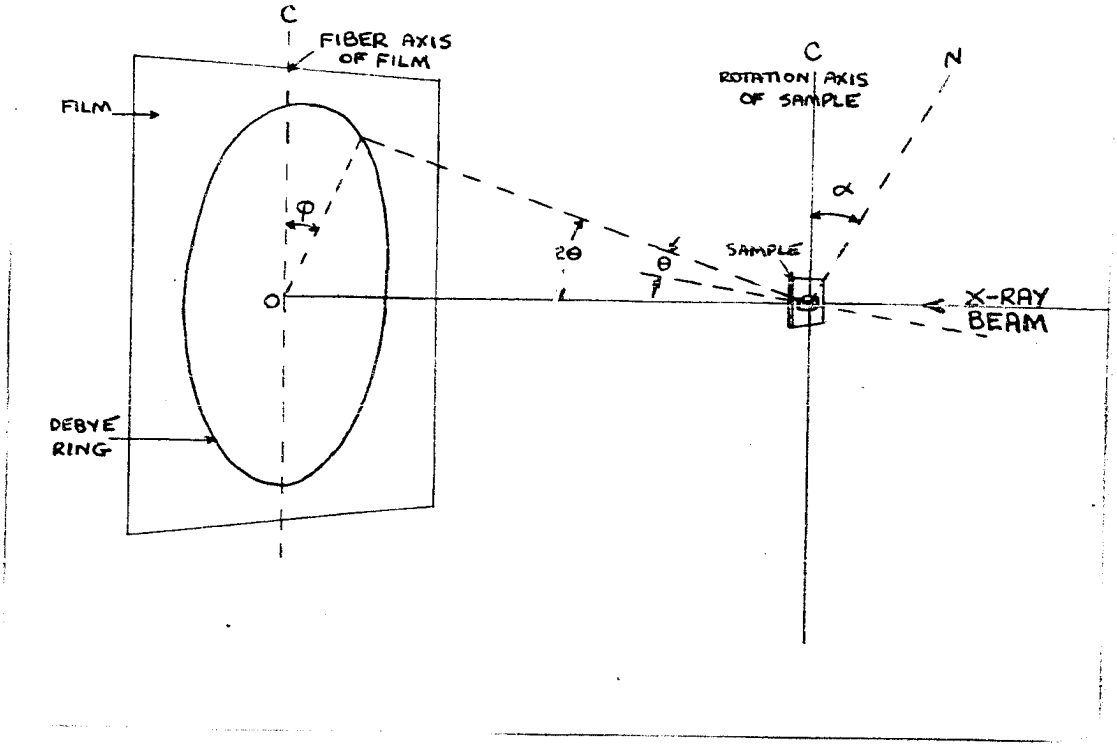

Figure 33. Showing the Interrelated Angles φ, α, and θ

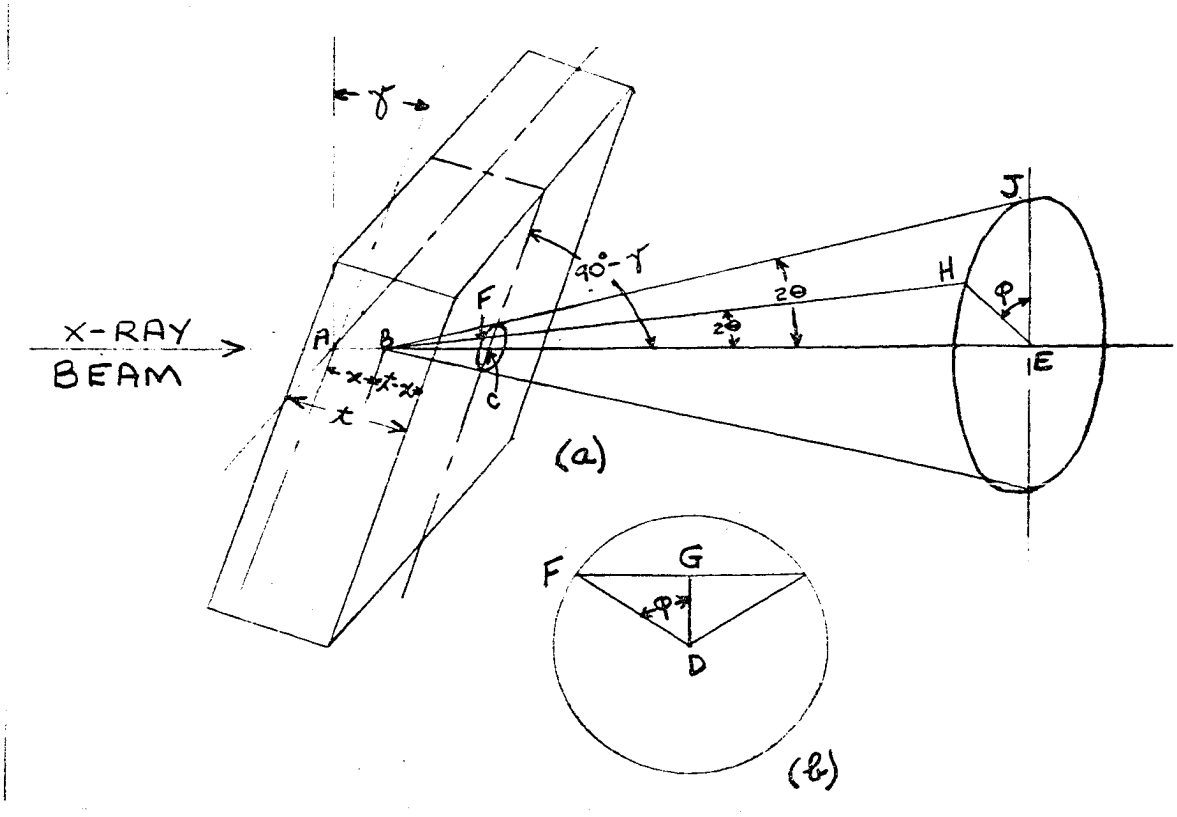

Figure 34. Sample With X-ray Beam Diffracted in Passing Through It

by stereographic projection of the data obtained for one set of crystal planes from a series of x-ray photographs taken with the sample at different angles to the x-ray beam. A pole figure is a circle which is the stereographic projection of an imaginary spherical surface at the center of which is placed a crystal.[10] Each point on the sphere is represented by a point on the projection, and each possible orientation of a plane in the crystal is represented by a point on the sphere (located at the intersection with the surface of the sphere of the normal to the plane which passes through the center of the sphere). Thus each point on the pole figure corresponds to definite orientation of a set of crystal planes being studied. For random orientation of the grains in the specimen, the pole figure will be of uniform low density. The pole figure of single crystal will contain regularly placed points of maximum density, with the remainder of the figure having zero density. The pole figure of a KCl crystal, worked as indicated earlier, shows by its varying density the extent and directions of deviations from ideal single crystal orientation.

Diffraction patterns obtained for different values of χ (the angle between x-ray beam and the normal to the surface of the sample) for a KCl sample, compressed at 50,000 lbs./in.^{2} and for 40 oscillations of the plunger, are shown in fig. 35-40.

Correction for Change in the Intensity due to Rotation of the Sample

Since the x-ray beam passed through the sample before falling on the photographic film, the intensity is decreased by absorption

X-RAY DIFFRACTION PATTERNS OF KCl SAMPLE (COMPRESSED AT 30,000 lbs./in.² FOR 40 OSCILLATIONS OF PLUNGER) ROTATED AT VARIOUS ANGLES ABOUT VERTICAL AXIS

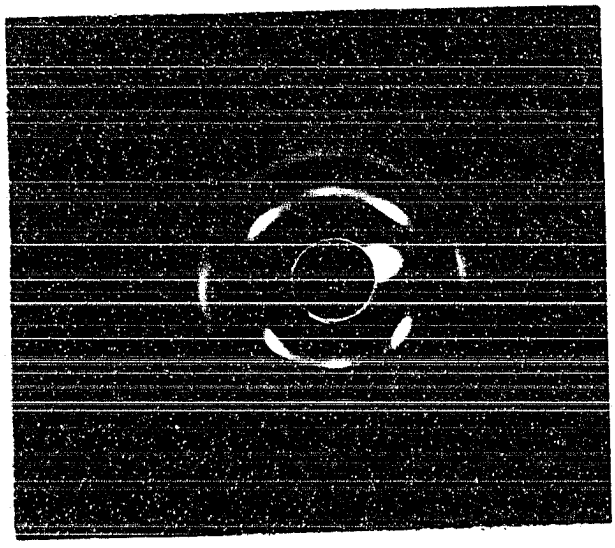

Figure 35. 0°

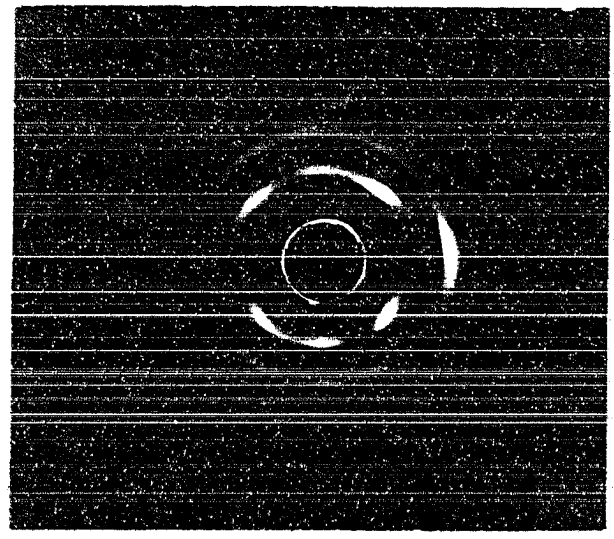

Figure 36. 10°

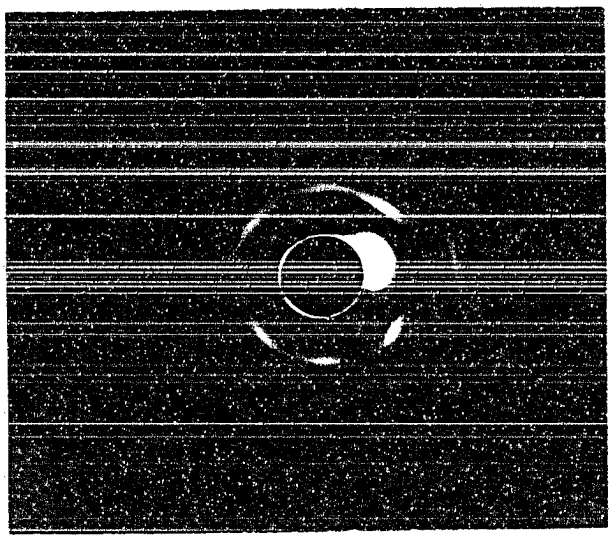

Figure 37. 20°

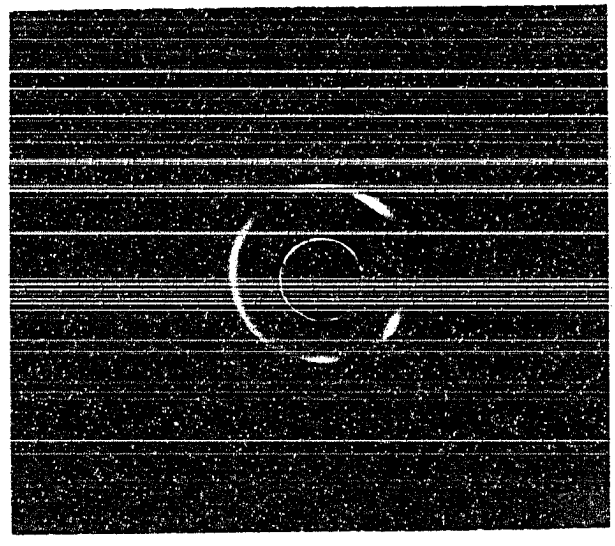

Figure 38. 30°

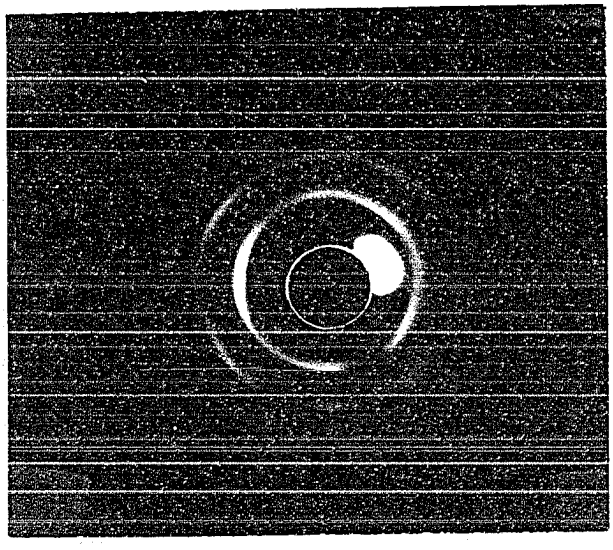

Figure 39. 40°

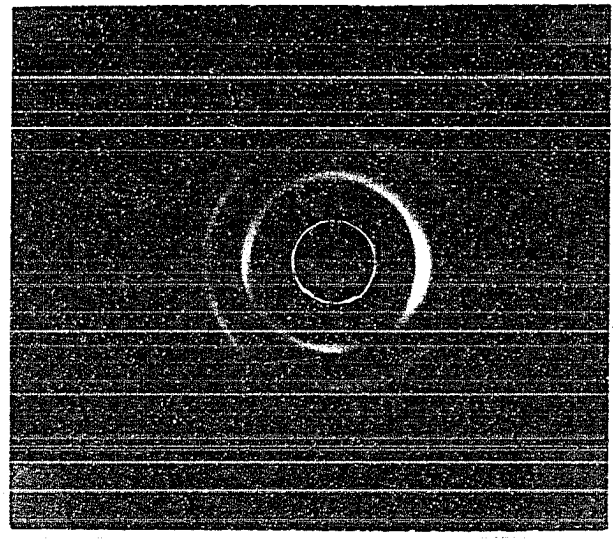

Figure 40. 50°

within the sample. With disk samples upon rotation, absorption is not the same for all the points on the Debye ring, since the diffracted rays traverse paths of unequal lengths. Maximum absorption occurs for the beam diffracted to the point of the Debye ring nearer portion of the sample inclined toward the film, while minimum absorption occurs for the beam diffracted to the opposite point of the Debye ring. The variation considered here is for random orientation and any variation due to preferred orientation is superimposed on this.

The correction for the change in intensity χ (the angle between the x-ray beam and the normal to the surface of the sample) is determined as follows.[10]

Fig. 34(a) shows the sample with the x-ray beam diffracted in passing through it. The sample is of thickness t, and makes an angle χ with the plane normal to the x-ray beam. Consider a ray ABFH, which is diffracted at B through an angle 2θ and strikes the film at H, the film being perpendicular to the direction of the original x-ray beam. The azimuth angle HEJ is denoted by Φ. C is the intersection with the sample surface of the direct x-ray beam, and F is the point where the ray under consideration intersects the surface. Fig. 34 (b) shows the Debye circle through F. The direct x-ray beam is perpendicular to the plane of the figure and passes through D; therefore the portion of this Debye circle above the horizontal line through F lies inside the sample, the lower portion lies outside, and the plane of the circle makes an

angle γ with the sample (that is angle BGC is γ). FD and GD in fig. 34 (b) are parallel to HE and JE, respectively, in fig. 34 (a). Thus angle FDG = φ.

Let d be the total distance traversed by the diffracted ray in passing through the sample. Then

$$d = AB + BF \quad (6) \qquad AB = \frac{x}{\cos\gamma} \quad (7) \qquad BF = \frac{BC + CD}{\cos 2\theta} \quad (8)$$

since GD is perpendicular to the direct beam ABCDE. Also

$$BC = \frac{t - x}{\cos\gamma} \quad (9) \qquad CD = GD \tan\gamma = FD \cos\varphi \tan\gamma$$

But FD is perpendicular to BCD, so that FD = BF sin 2θ. Therefore

$$CD = BF \sin 2\theta \cos\varphi \tan\gamma \quad (10)$$

Combining (8), (9), and (10), we get

$$BF = \frac{\frac{t - x}{\cos\gamma} + BF \sin 2\theta \cos\varphi \tan\gamma}{\cos 2\theta} \quad \text{or} \quad BF = \frac{t - x}{\cos\gamma\cos 2\theta - \sin\gamma\sin 2\theta \cos\varphi} \quad (11)$$

From equations (6), (7), and (11)

$$d = \frac{x}{\cos\gamma} + \frac{t - x}{\cos\gamma\cos 2\theta - \sin\gamma\sin 2\theta \cos\varphi} \quad (12)$$

The intensity at H due to the ray ABFH will be

$$I_\varphi(x) = I_0 e^{-\mu d} \quad (13) \qquad \text{where}$$

μ = coefficient of absorption of the material

I_0 = constant depending on the initial intensity of the x-ray beam and the fraction of the original beam that is diffracted

To get the total intensity at H, this function must be integrated

from x = 0 to x = t, since rays are diffracted to H from all points along AC. Thus,

$$I_\varphi = I_o A \int_o^t e^{Bx} dx = I_o \frac{A}{B} (e^{Bt} - 1) \qquad (14)$$

where

$$A = e^{-\mu t C} \qquad B = -\mu\left(\frac{1}{\cos\chi_0} - C\right) \qquad C = \frac{1}{\cos\chi_0 \cos 2\theta - \sin\chi_0 \sin 2\theta \cos\varphi}$$

If I_φ is the intensity at φ on a particular χ_0 film and is given by

$$I_\varphi = I_o \frac{A_\varphi}{B_\varphi} (e^{B_\varphi t} - 1)$$

and I_π is the maximum intensity for the same χ_0 film (π is the point on the film away from the inclination of the sample) and is given by

$$I_\pi = I_o \frac{A_\pi}{B_\pi} (e^{B_\pi t} - 1)$$

then the correction for the absorption can be found from

$$\frac{I_\varphi}{I_\pi} \times 100 \qquad (15)$$

Fig. 41 shows the graph of $I_\varphi / I_\pi \times 100$ as a function of the azimuthal angle φ for the 100 reflections ($\theta = 6.46^\circ$) and for two values of χ_0 of 30° and 60°. Note increase of absorption for larger values of χ_0. Fig. 42 shows the same graph plot for the 110 reflections ($\theta = 9.15^\circ$) for values of χ_0 of 30° and 50°. As can be seen by comparing $\chi_0 = 30^\circ$ for both graphs, there is more absorption for the 110 reflections than for the 100 reflections.

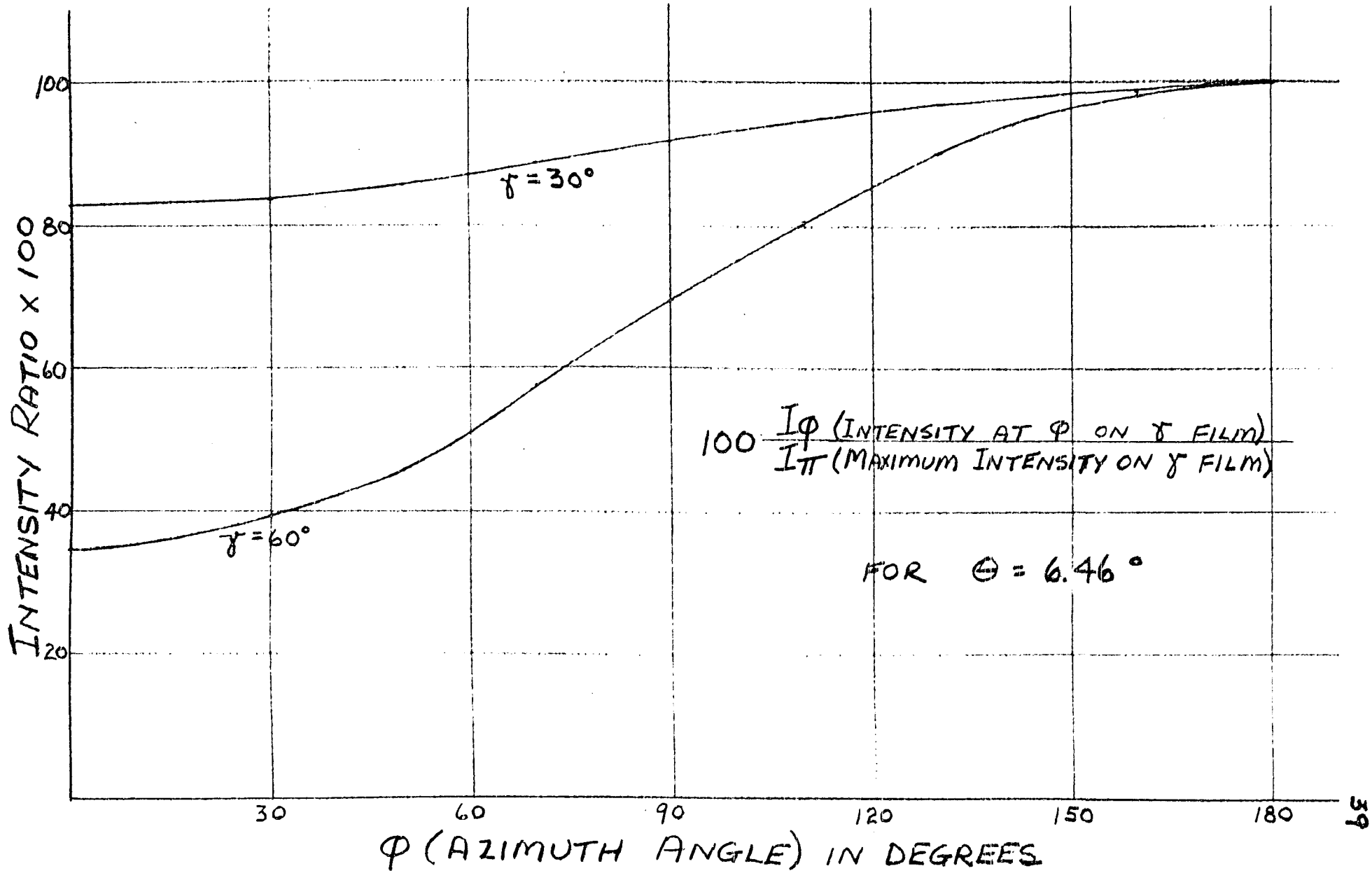

FIGURE 41

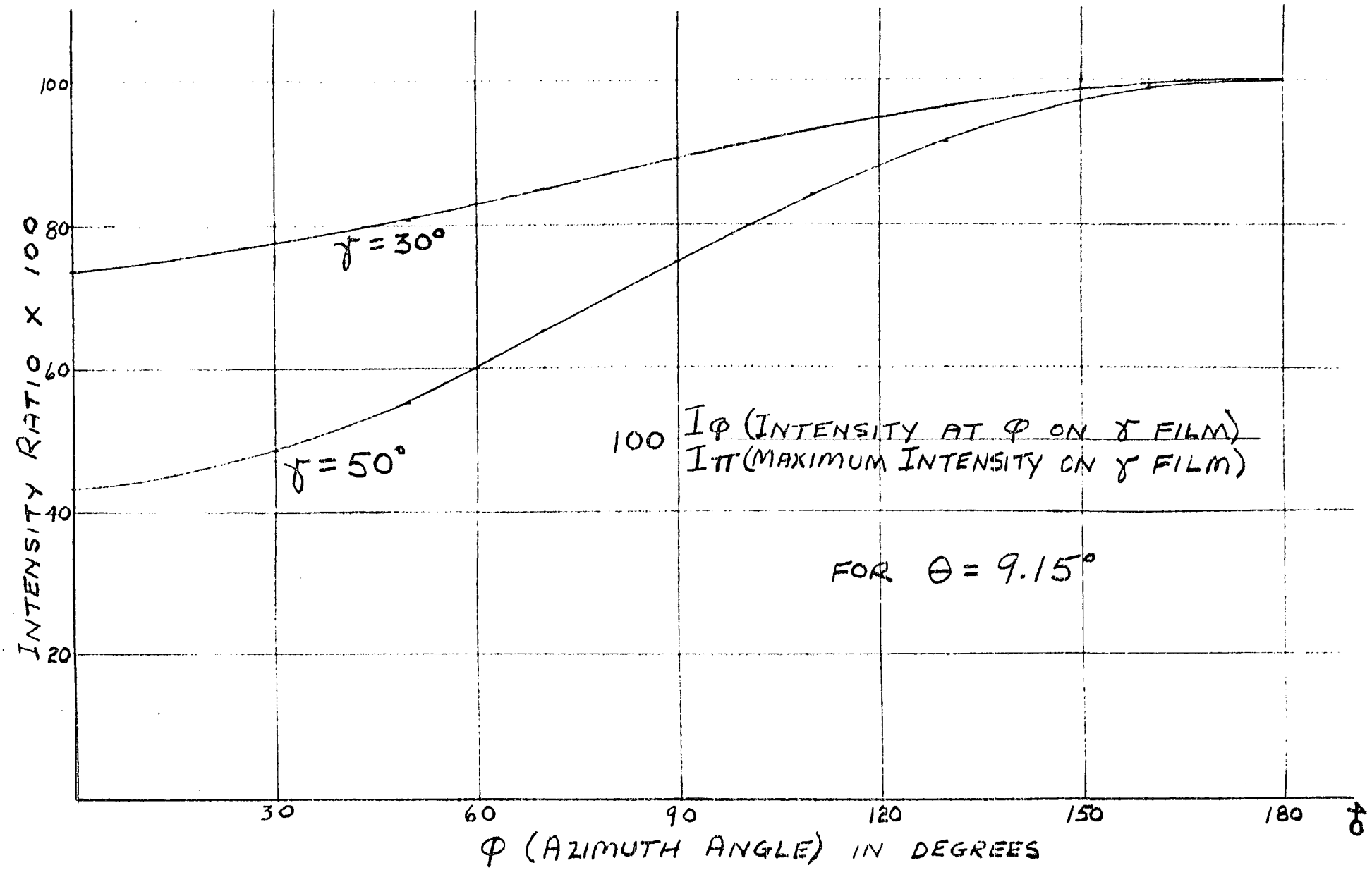

FIGURE 42

Construction of Pole Figure Chart

The labor of plotting a pole figure is made easier if a chart is made up in which the series of reflection circles are shown the position they would have after rotation back to the setting which makes the plane of specimen coincide with the plane of the basic circle. A different chart is required, of course, for every different value of θ that is used, thus for different wavelengths, for different specimen materials, and different reflecting planes. The pole figure charts were made in the following manner.[10]

A standard stereographic net (14 cm. in diameter) of size desired for pole figure was chosen (fig. 43). A piece of fairly transparent paper was placed over the net and onto it was traced the equator, vertical meridian, and the boundary circle of the net.

The data obtained from the proper Debye ring on the 0° film; ie., the film taken with the specimen at right angles to the undeviated x-ray beam, was recorded on a circle known as the 0° reflection circle. This circle must be concentric with the boundary circle of the pole figure and was drawn with a radius of $90 - \theta$ degrees as measured on the equator of the net.

For the determination of the parallels of latitude for the pole figure chart, each quadrant of 0° circle just constructed was divided into 10° arcs by drawing radial lines at 10° intervals and extending them to the boundary circle. The intersections of the radial lines with the 0° circle represented points where the 10°

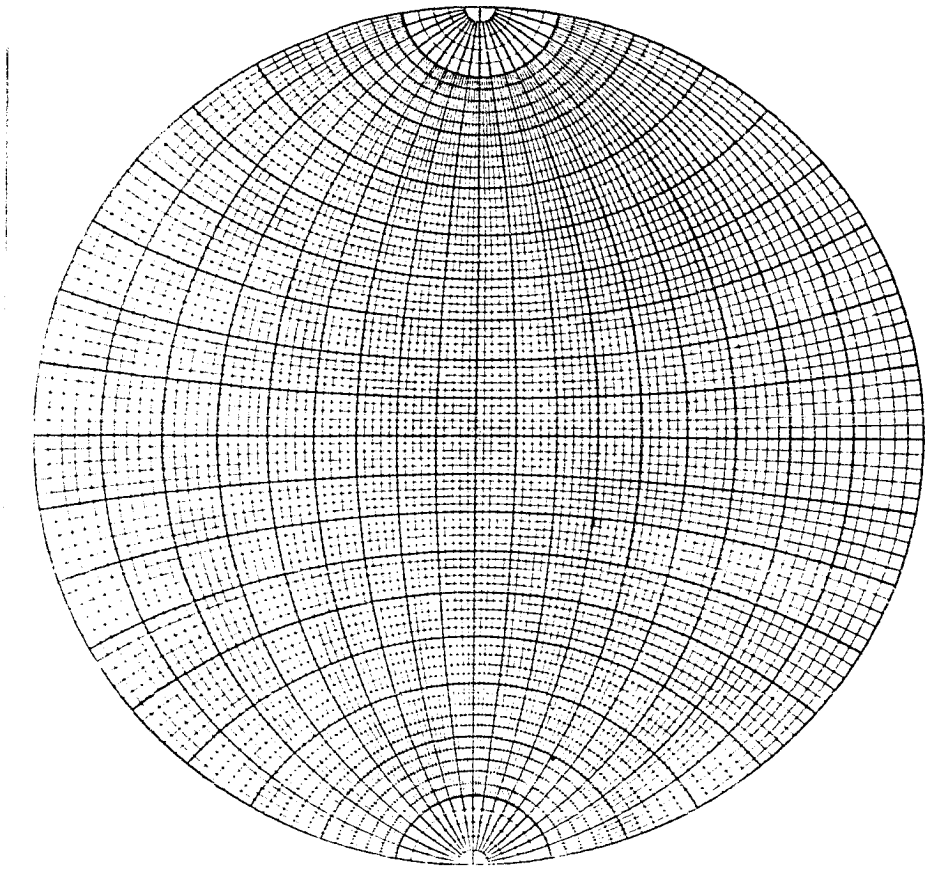

Figure 43. Stereographic Net, Wulff or Meridianal Type

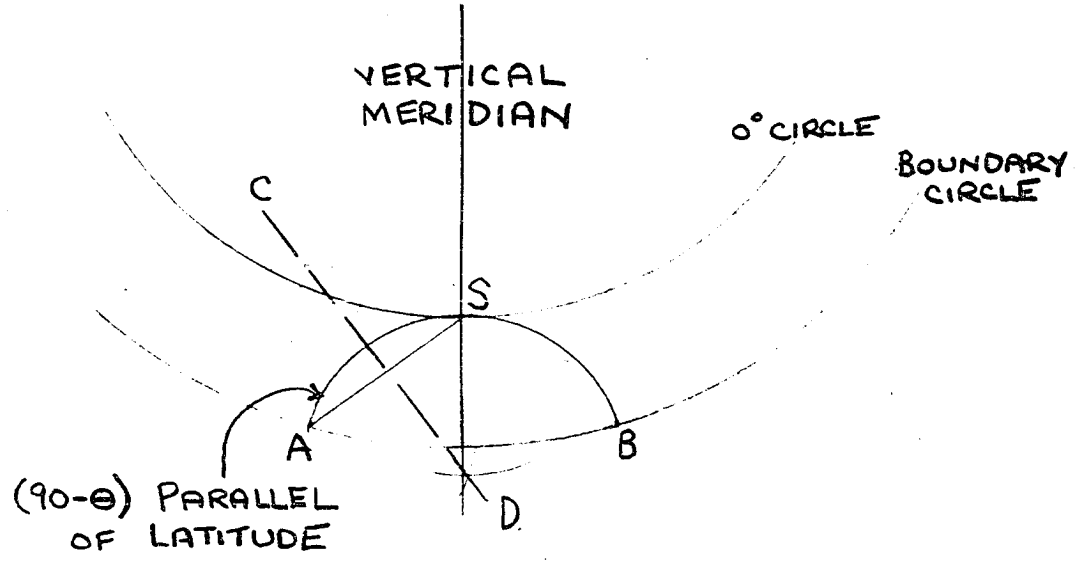

Figure 44. Construction of Tangent Circle

parallels of latitude for the pole figure chart cut the 0° circle. These parallels of latitude were drawn in, complete to the boundary circle, by tracing them from those of the stereographic net.

At the north and south poles of 0° circle, it was desired to construct tangent circles which contained the $90 - \theta^{\circ}$ parallels of latitude of the net. This was done as follows. By the rules of stereographic projection the center of these tangent circles must be on the extended vertical meridian. The perpendicular bisector of line SA, fig. 44, which is drawn from pole, S, of the 0° circle to the intersection, A, of the $90 - \theta^{\circ}$ parallels of latitude of net with the boundary circle and thus is a chord of the tangent circle, must pass through the center of the desired circle. Therefore point R, where the perpendicular intersects the vertical meridian, is the center of the desired tangent circle.

For the case of the 0° reflection circle, the plane of the Debye ring on the film is parallel to the plane of the sample. Now suppose the sample is rotated through n° about an axis represented by the vertical meridian on the pole figure chart. Although the Debye ring is still circular, it is no longer parallel to the sample. The fact that the stereographic projection of a circle is a circle, the n° film data will be recorded on circles. When the inclination of the sample to the film is such as to throw a portion of the circle outside the boundary circle, the data will be recorded on circular arcs, one representing the portion within the boudary circle and the other the reflection of the portion which lies outside the boundary.

These were determined as follows.

By stereographic projection rules, centers of all circles must lie on the equator (or equator extended). In left half, one circle intersects equator at points located n° to the right of the 0° circle, as measured on the net. In the right half of the chart, n° may exceed the number of degrees on the equator of the net to the right of the 0° circle, in which case the desired point is found by retracing the path along the equator from the boundary circle to the left for a degree distance equal to the difference between n° and the number of degrees on the equator of the net between the 0° circle and the boundary circle. Thus it is evident that when it is necessary to retrace the path to locate the intersecting point on the equator, the result is two circular arcs instead of a complete circle.

Theory of stereographic projection requires that the circle (or circular arcs) be tangent to each of the tangent circles. Point of tangency is located at a point n° to the right of the vertical meridian, as determined by the intersection of the n° radial lines of the tangent circle with its periphery. When these three points (point of intersection on the equator and points of tangency with the tangent circles) are found, the center of the n circle can be determined in similar manner that was used in finding the centers of the tangent circles. In the case of two circular arcs, the left arc is constructed first, and the intersections it makes with the boundary circle along with proper point on the equator are

used to determine the center ofthe right arc. The other n° reflection circle is located in a similar manner to the left of the 0° circle.

Fig. 45 shows a pole figure chart which was constructed over a stereographic net and net removed for the 100 planes of the KCl sample. Fig. 46 shows a similar pole figure chart for the 110 planes of the KCl sample for the same MoK$_\alpha$ radiation. As can be seen from the charts, reflection circles at intervals of 10° were drawn.

Construction of Pole Figure

Upon the completion of the pole figure chart for the proper θ and the necessary number of diffraction patterns of the sample taken, the construction of the pole figure is possible.

First the film must be interpreted for the necessary data in the following way. The intensity distribution around the circle is determined by the use of a 5-zone rating (0, 1, 2, 3, and 4 where 0 indicates zero intensity and 4 indicates maximum intensity). The zone boundaries are recorded in degrees with respect to some reference point on the Debye circle with the use of a polar net. Absorption corrections had to be made for the variation around the Debye circle on the film.

To make a pole figure, tracing paper was placed over the pole figure chart and on it was traced the boundary circle.[10] The data taken from each film as described above must be recorded on the proper reflection circles of the pole figure chart. Consider for example the KCl 30° film for the 110 planes. Data from this film

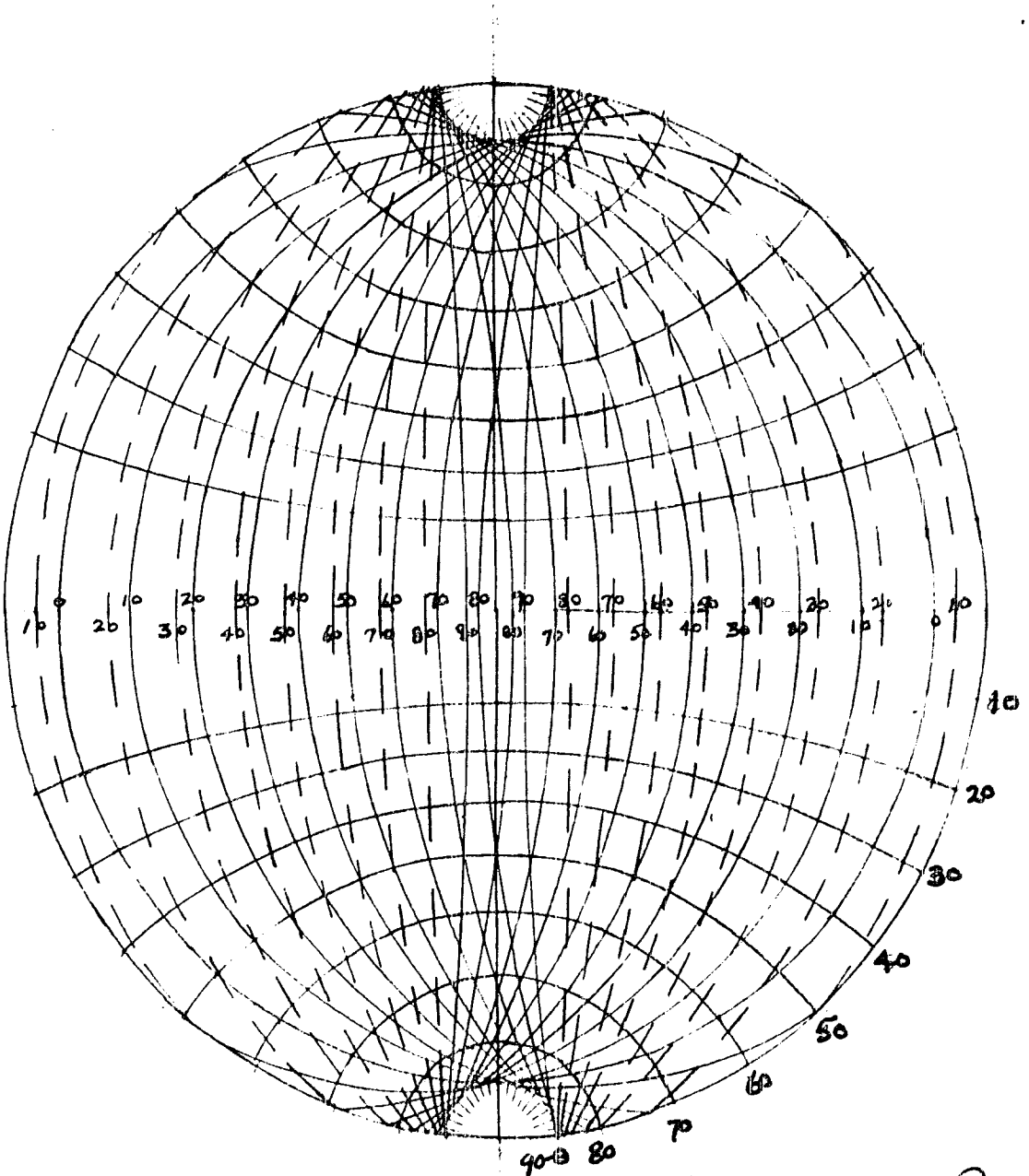

FIG. 45 POLE-FIGURE CHART FOR MoKα RADIATION REFLECTING FROM (100) PLANES OF KCl SAMPLE ($\theta = 6.46°$)

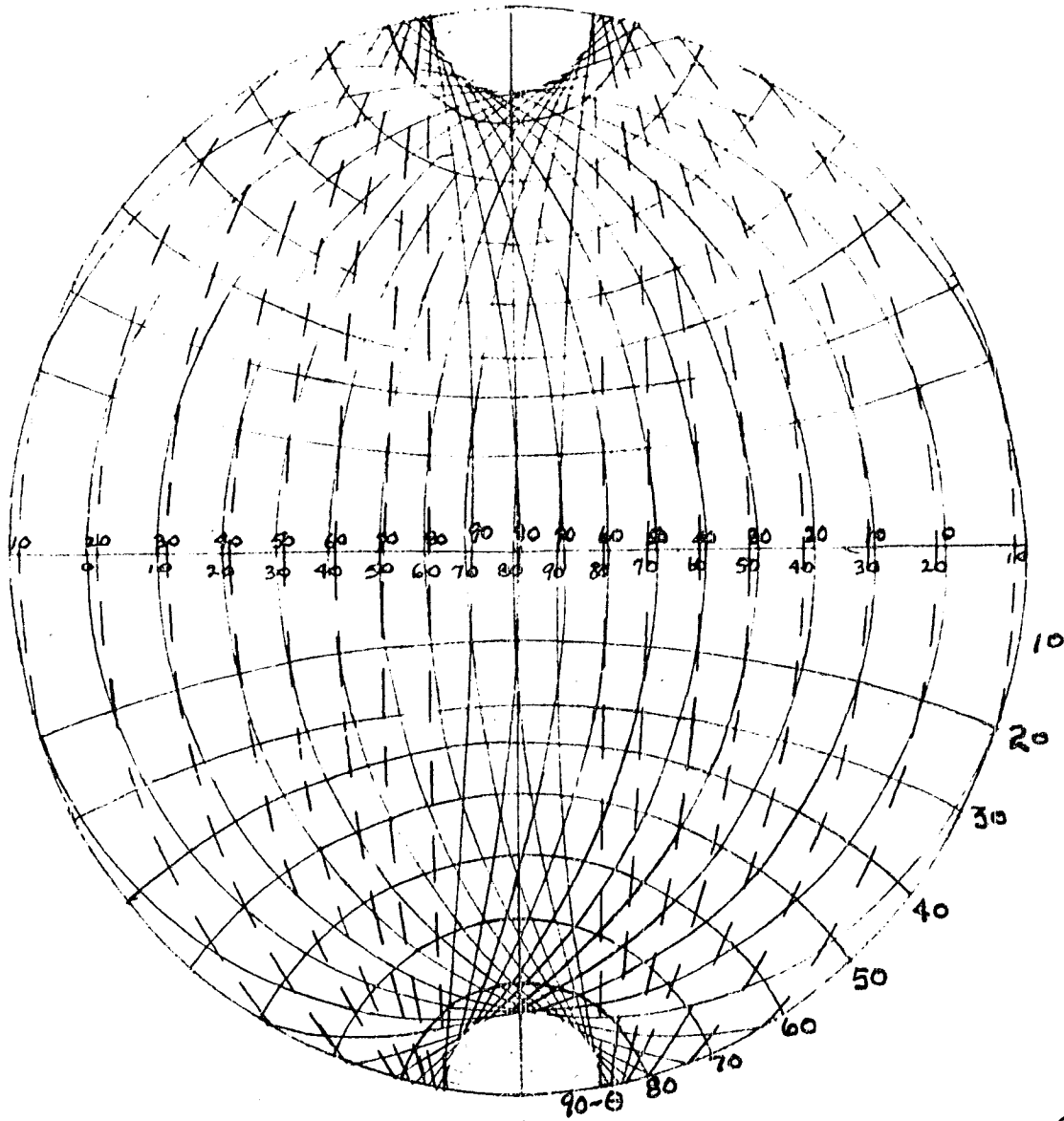

FIG. 46. POLE FIGURE CHART FOR MoKα RADIATION REFLECTING FROM (110) PLANES OF KCl SAMPLE (θ=9.15°)

must be recorded on the 30° reflection circles (see fig. 47). The direction of reference selected is marked 0° and corresponds to the point A on the pole figure. On the film there is a region of intensity 1 for 20° on either side of 0°, therefore for 20° either side of A on 30° circle of the pole figure, there is a region of intensity 1, and is marked with a dashed line, according to the scale of differentiation shown in fig. 47. Boundaries of this 1 intensity zone are also boundaries of 2 intensity zones whose other boundaries lie 35° on either of 0°. On the pole figure these boundaries lie 35° on either side of A, and the region between the boundaries of 2 intensity zones are marked with plus signs as designated for intensity 2 on the scale of differentiation. These regions are bounded by 3 intensity zones to 60° on either side of A, etc., until the arc is completed.

Starting from A' instead of A, the same data is recorded around arcs A'B'C'D'A'. The arcs designated by prime letters correspond to a film taken with the angle of rotation of the sample n° in a direction opposite to that for which film shown above was taken. Data for each film was recorded in the same manner on the corresponding reflection circles.

It is noticed that the diffraction pattern is symmetrical to both the vertical and horizontal directions for the 0° film. But as the sample is rotated around the vertical direction, the pattern becomes more and more unsymmetrical with respect to the vertical direction but retains its symmetry to the horizontal or shear direction.

After all of the data has been recorded on the pole figure, like

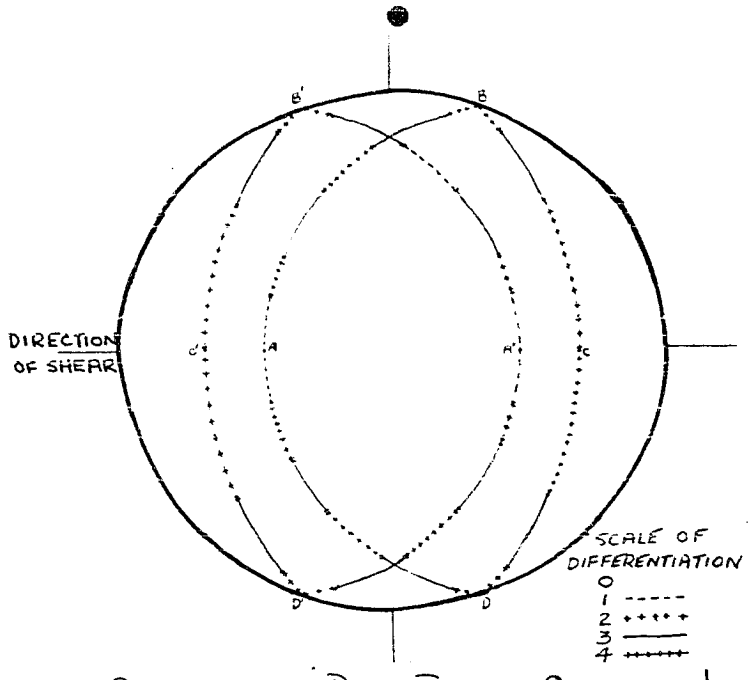

FIG. 47. RECORDING ON POLE FIGURE CHART OF INTENSITIES DATA TAKEN FROM 30° FILM FOR (110) REFLECTIONS

zone boundaries are joined with smooth curves. The pole figure is thus divided into different intensity zones. The interpretation of these were simplified with the filling in of the zones with different cross-hatching.

Pole figures for the 100 and the 110 planes of the KCl sample, compressed with oscillation of the plunger in the manner described earlier, are shown in fig. 48 and fig. 49 respectively.

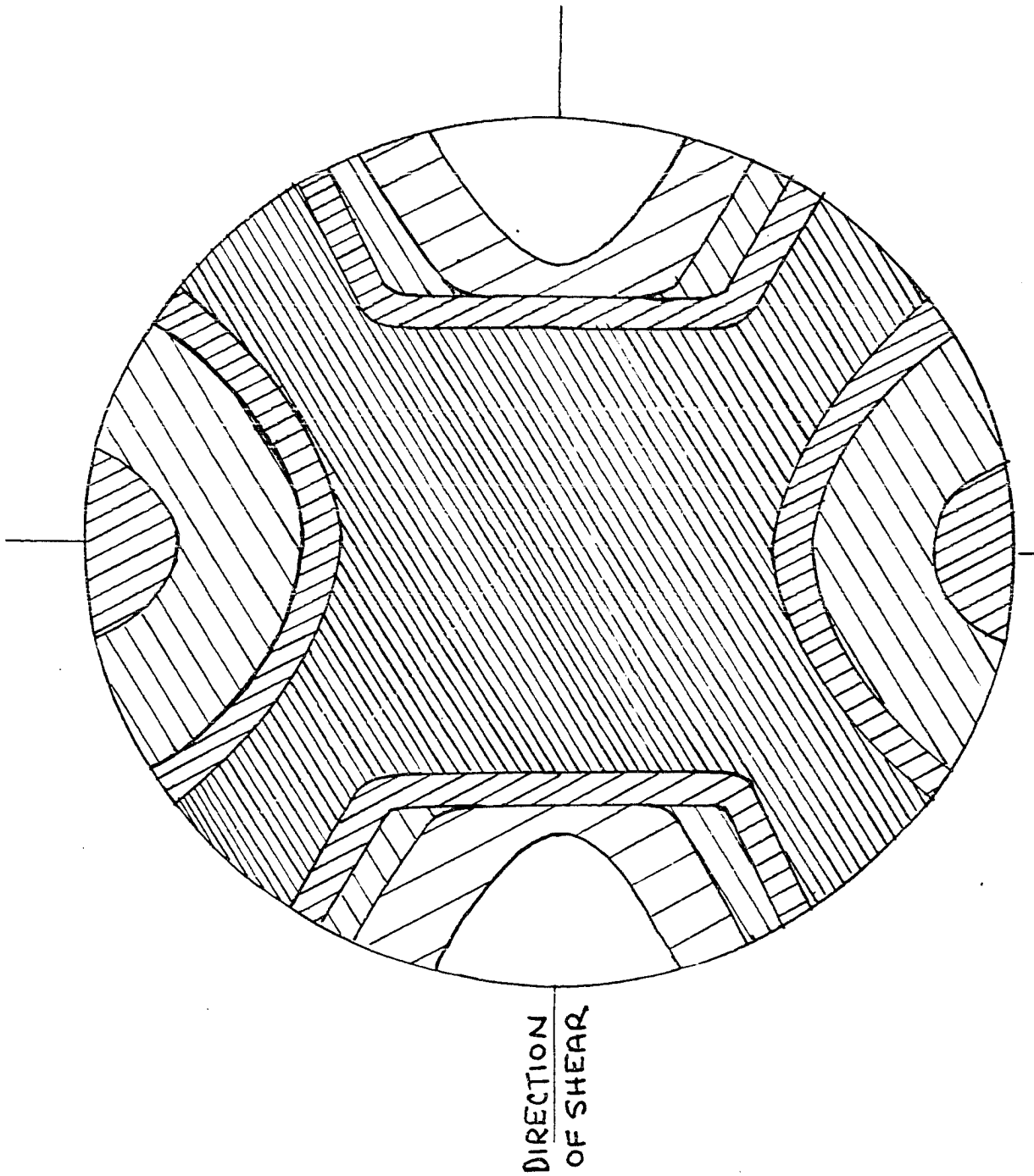

FIG. 48. (100) POLE FIGURE FOR KCl SAMPLE

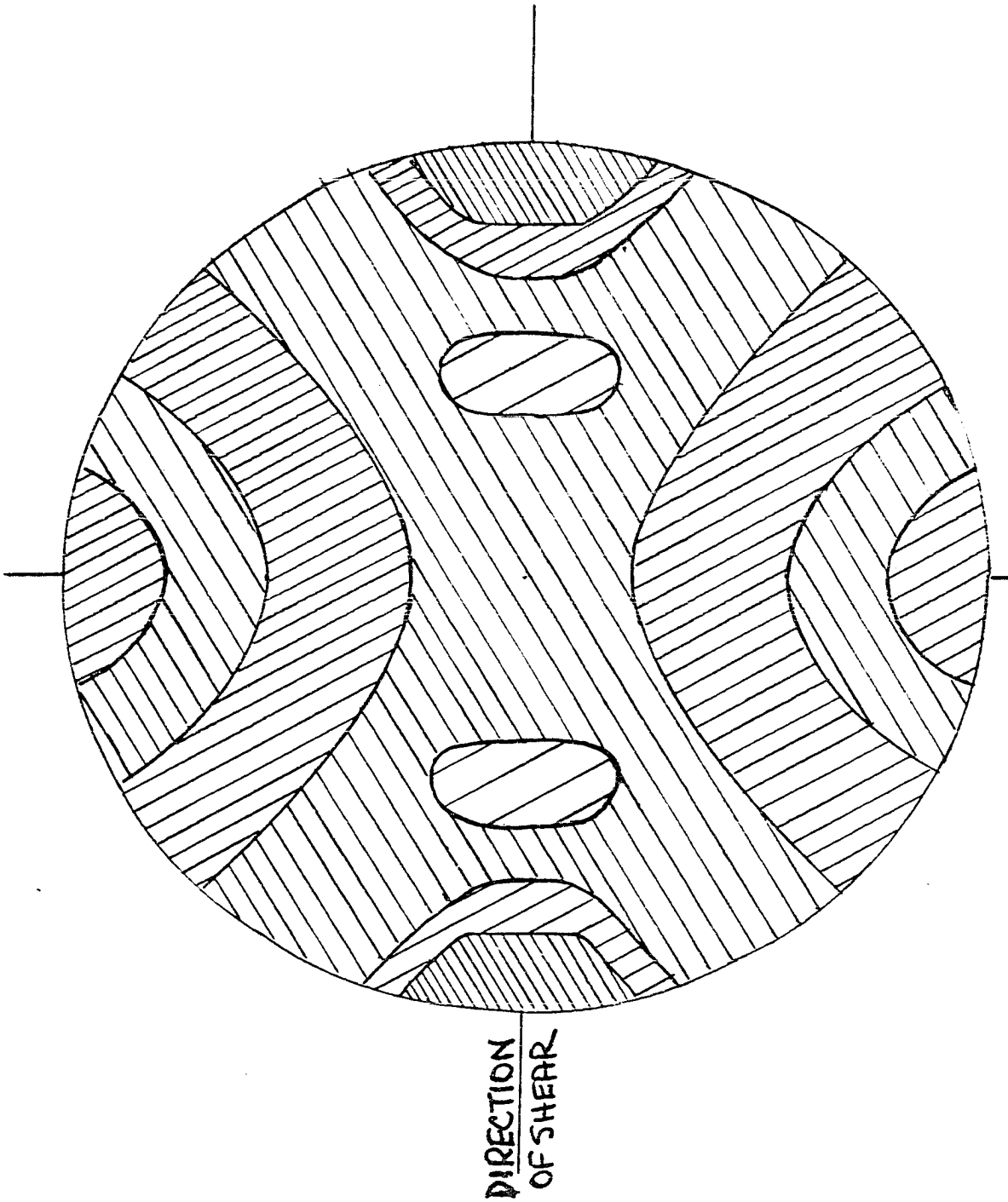

FIG. 49. (110) POLE FIGURE FOR KCl SAMPLE

INTERPRETATION OF POLE FIGURES

A general scheme for interpreting pole figures will be explained, followed by specific results from the pole figures obtained for this case. The equator of the pole figure corresponds to the direction of shear. The orientations of the normals to the planes under consideration which give rise to various spots on the pole figure may be found as follows. Determine the colatitude, n°, of the spot, and the meridian angle, m°, (where $m \leq 90^{\circ}$) between the spot and the boundary circle of the pole figure. The normal to the planes responsible for this spot will make an angle n° to the north-south direction (perpendicular to the shear direction).

From the above, rules for specific points may be written down.[10]

A. Central point of the pole figure - normal to the crystal planes is perpendicular to the plane of the specimen.

B. Points on the circumference of the pole figure - normal to the crystal planes lies in the plane of the specimen.

   a. Points at the north and south poles - normal to the crystal planes lies perpendicular to the direction of shear.

   b. Points on the equator - normal to the crystal planes lies parallel to the direction of shear.

   c. Points with colatitude n° - normal to the crystal planes makes an angle n° with the north-south direction.

C. Points on the equator m° from the boundary circle - normal to the

crystal planes is perpendicular to the north-south direction and makes an angle of m° to the direction of shear.

D. Points on the vertical meridian with colatitude n° - normal to the crystal planes is perpendicular to the direction of shear and makes an angle n° to north-south direction.

Pole figure for the 100 planes shows a not too concentrated maximum intensity band spreading across pole figure at $\pm 35^{\circ}$-55° colatitude to north-south direction, with fairly concentrated intensity bands spreading across figure at $\pm 10^{\circ}$ colatitude and $\pm 30^{\circ}$ - 35° colatitude to north-south direction.

Pole figure for the 110 planes reveals a very concentrated maximum intensity band at $\pm 15^{\circ}$ to direction of shear, with less concentrated intensity bands spreading across pole figure at $\pm 10^{\circ}$ colatitude and $\pm 25^{\circ}$ - 45° colatitude to the north-south direction.

COMPARISON OF PREFERRED ORIENTATION FOR NaCl, KCl, and KBr POWDERED CRYSTALS

The x-ray diffraction patterns for NaCl, KCl, and KBr samples compressed with oscillation of the plunger under same conditions are shown in fig. 50-52. As indicated by the patterns, NaCl shows the least degree of preferred orientation, followed by KCl and KBr in that order.

It is believed that the above result (tendency of some crystals to show a greater degree of preferred orientation for the same conditions than others) is correlated with the lattice energies of the crystals.

Born and Mayer have established a calculation of the lattice energies upon a rather firm basis.[13] Their expression for the energy per gram molecule is

$$U(r) = \left(-\frac{\alpha e^2}{r} - \frac{C}{r^6} + B(r) + \epsilon \right) N$$

where α is the Madelung constant (1.747)

C is a constant such that C/r^6 represents the effect of the Van der Waals forces of attraction

B(r) is a complex exponential expression based on the assumption of a potential due to a repulsive force between two ions

ϵ is the zero-point energy of the lattice and is equal to $9/4\ h\nu_{max}$ where ν_{max} is the highest frequency of oscillation associated with the lattice

e^2/r is the electrostatic energy which disappears as ions come together

X-RAY DIFFRACTION PATTERNS OF NaCl, KCl, and KBr SAMPLES

(COMPRESSED AT 50,000 lbs./in.^{2} WITH 40 OSCILLATIONS OF PLUNGER)

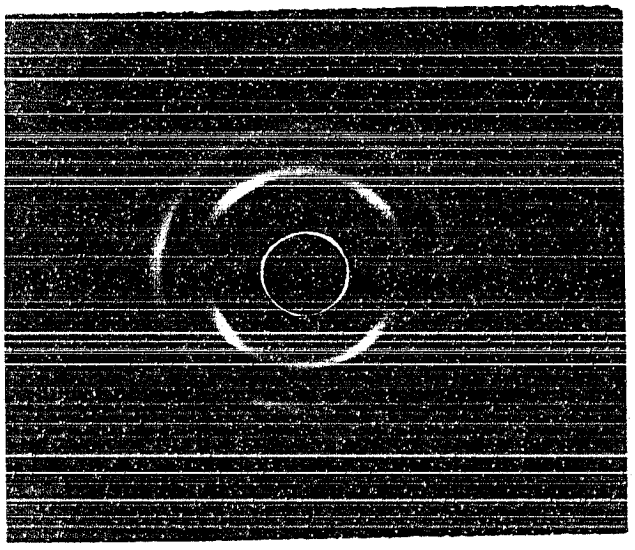

Figure 50. NaCl

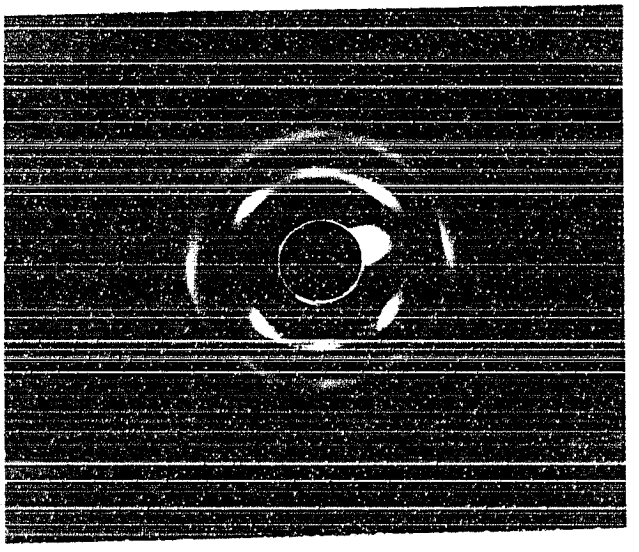

Figure 51. KCl

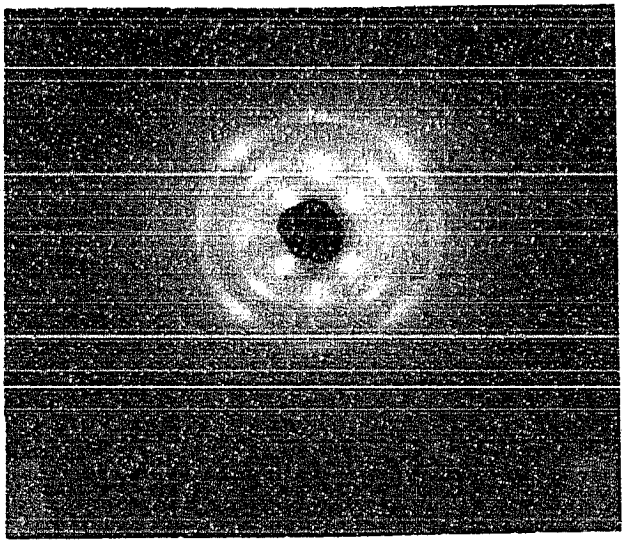

Figure 52. KBr

Mayer and Helmholtz calculated the lattice energies of the above alkaline halides on this basis and their results for the energy per gram molecule in K. cal. per gram-atom are NaCl (183.1), KCl (165.4), and KBr (159.3). These agree with pattern results. It was noticed in some of the preliminary experimentation that KBr had a greater tendency to clear up at lower pressures than that required for the others. In fact a completely clear sample of NaCl was not obtained with this apparatus.

SUMMARY OF RESULTS

It was possible in this investigation to obtain completely transparent samples of KCl powder compressed in a vacuum. These resulted either by the application of high pressure alone (around 125,000 lbs./in.^{2}) to the powdered KCl or by the application of a lower pressure (around 40,000 lbs./in.^{2}) accompanied by oscillation of the plunger piece of the die. It seems therefore that the oscillatory motion of the plunger served to fill in the microscopic voids more effectively than the compression alone.

The x-ray diffraction patterns of KCl samples ranged from a very spotty ring pattern for no pressure to a sharp ring pattern for a pressure of 10,000 lbs./in.^{2}, indicating a decrease in the grain size from between 60-80 microns to slightly less than 5×10^{-3} mm. X-ray diffraction patterns of samples compressed from 10,000 lbs./in.^{2} to 200,000 lbs./in.^{2} showed no changes. This is clearly indicated by the microphotometer tracings of fig. 17-19. Therefore, the grain size of KCl samples compressed from 10,000-200,000 lbs./in.^{2} must lie in "sharp ring" pattern range between 5×10^{-3} mm. to 2×10^{-4} mm. Since the Debye rings retained uniform density throughout this phase of the investigation, it appears that no preferred orientation prevailed in the samples with compression only.

X-ray diffraction patterns of KCl compressed with oscillation of the plunger piece of the die revealed that the oscillatory motion

introduced a preferred orientation in the sample, ie., a tendency of the crystals to align themselves. The patterns indicated that an increase of pressure up to 50,000 lbs./in.^{2} for a constant number of oscillations of the plunger or an increase in the number of oscillations of the plunger up to 40 for a constant pressure both served to increase the degree of preferred orientation.

A study of this preferred orientation revealed that the 110 axes of the sample tended to align themselves parallel to the direction of shear. A more detailed description of the lining up of the planes was obtained through the construction of pole figures for the 100 and 110 planes. The pole figure for the 100 planes showed a not too concentrated maximum intensity band spreading across the pole figure at approximately $\pm 35^\circ$-55° colatitude to north-south direction, with fairly concentrated intensity bands spreading across figure at ± 10 colatitude and $\pm 30^\circ$ - 55° colatitude to north-south direction. Pole figure for the 110 planes revealed a very concentrated maximum intensity band at $\pm 15^\circ$ to direction of shear, with less concentrated intensity bands spreading across pole figure at $\pm 10^\circ$ colatitude and $\pm 25^\circ$-45° colatitude to north-south direction.

A comparison of the diffraction patterns for NaCl, KCl, and KBr samples all compressed at 50,000 lbs./in.^{2} and for 40 oscillations of the plunger revealed a greater degree of preferred orientation for KBr, followed by KCl and NaCl in that order. A comparison of lattice energies for these three crystals showed the energy per gram molecule for NaCl greater than KCl or KBr (in that order). Therefore, there

seemed to be a correlation between the lattice energies for certain crystals and the degree of preferred orientation obtained for these same crystals under the same conditions.

ACKNOWLEDGEMENTS

To Dr. D.A. Wells for having suggested this problem and for his assistance throughout the work, to Mr. Allan Chase for having constructed the apparatus and forhis assistance with the technical details, and to Dr. Fred O'Flaherty and Department of Tanning Research for the use of their X-ray diffraction machine, the writer wishes to express his gratitude and deepest appreciation.

REFERENCES

1. G.L. Clark and M.M. Beckwith; Transactions, American Society for Metals, vol. 25, 1937, pp 1207-1222.

2. C.F. Elam; "Distortion of Metal Crystals", Clarendon Press, Oxford, 1935.

3. H. Mark, M. Polanyi, and M. Schmid; Zeitschrift fur Physik, vol. 12, 1923, p 58.

4. P.W. Bridgman; Journal of Applied Physics, 18, No. 2, 1947, pp 246-256.

5. W.T. Sproull; "X-Rays in Practice", McGraw-Hill, 1946, p 440.

6. W.D. Jones; "Powder Metallurgy", Edward Arnold and Co., London, 1937, p 34.

7. M. Field; "Studies in the Physics of Metal Cutting", Doctor's Thesis, U. of Cincinnati, 1948, p 73.

8. M.F. Goss; Transactions, American Society for Metals, vol. 23, 1935, p 511.

9. J.L. Snoek; Zietschrift Metallkunde, vol. 30, 1938, p 94.

10. B.F. Decker; Proceedings of American Society for Testing Materials, vol. 43, 1943, pp 785-802.

11. A. Taylor; "An Introduction to X-Ray Metallography, John Wiley and Sons, 1945, pp 266-269.

12. R.M. Bozorth; Physical Review, No. 26, 1925, p 390.

13. W.H. Bragg, and W.L. Bragg; "The CrystallineState", vol. 1, MacMillan Co., 1934, p 196.

14. C.S. Barrett; "Structure of Metals", McGraw-Hill, 1943.

15. G.L. Clark; "Applied X-Rays", McGraw-Hill, 1940.

16. R.W.G. Wyckoff; "The Structure of Crystals", Chemical Catalog Co., 1931.

17. A.H. Compton and S.K. Allison; "X-Rays in Theory and Experiment", D. van Nostrand Co., 1935.

18. C.W. Bunn; "Chemical Crystallography", Clarendon Press, Oxford, 1945.

19. A.H. Compton; "X-Rays and Electrons", D. van Nostrand Co., New York, 1926.

20. H. Hirst; "X-Rays in Research and Industry", Chemical Publishing Co., Brooklyn, 1943.